

# Wetland Mapping Methods for the Twin Cities Metropolitan Area

---

Joseph F. Knight, Ph.D.  
Jennifer Corcoran, M.S.  
Lian Rampi  
Bryan Tolcser  
Margaret Voth

Remote Sensing and Geospatial Analysis Laboratory  
Department of Forest Resources  
University of Minnesota

6/18/2009



## Contents

1. Introduction .....	4
1.1. Objectives.....	4
1.2. Background .....	4
1.2.1. Classification Methods.....	5
1.2.2. Multitemporal Data .....	6
1.2.3. Hyperspectral Data .....	7
1.2.4. Radar Imagery.....	7
1.2.5. Ancillary Data Sets .....	8
2. Methods/Results.....	10
2.1. Wetland Mapping using Terrain Indices .....	10
2.1.1. Terrain Indices Introduction.....	10
2.1.2. Terrain Indices Methods .....	10
2.1.3. Terrain Indices Results .....	15
2.1.4. Terrain Indices Discussion.....	22
2.1.5. Terrain Indices Conclusions.....	23
2.2. Wetland Mapping using Object Oriented Algorithms .....	24
2.2.1. Introduction to Object-Oriented Classification.....	24
2.2.2. Segmentation Methodology .....	25
2.2.3. Pilot Segmentation Results .....	27
2.2.4. Segmentation Discussion .....	31
2.3. Wetland Typing using Decision Trees .....	32
2.3.1. Wetland Typing Introduction.....	32
2.3.2. Wetland Typing Methods.....	32
2.3.3. Wetland Typing Results.....	35
2.3.4. Wetland Typing Discussion .....	41
2.3.5. Wetland Typing Conclusions.....	42
2.4. Wetland Mapping using RADAR Imagery.....	42
2.4.1. Introduction to Wetland Mapping with Radar Imagery .....	42
2.4.2. Planned Methodology.....	43
2.4.3. Expected Results .....	45
2.4.4. RADAR Summary and Conclusions.....	45
2.5. Field Wetland Data Collection in Carlton County .....	46
3. Recommendations and Protocol for Wetland Mapping in the Metro Area .....	47
3.1. General Recommendations .....	47

3.2.	Mapping Protocol .....	48
3.2.1	Data Types and Software .....	48
3.2.2	Preprocessing .....	49
3.2.3	Data display and Interpretation .....	49
3.2.4	Data Post-processing and Delivery .....	49
3.2.5	Quality Assurance / Quality Control .....	50
4.	Conclusions .....	50
5.	References .....	51

Funding for this project was provided by the Minnesota Environment and Natural Resources Trust Fund as recommended by the Legislative-Citizen Commission on Minnesota Resources (LCCMR). The Trust Fund is a permanent fund constitutionally established by the citizens of Minnesota to assist in the protection, conservation, preservation, and enhancement of the state’s air, water, land, fish, wildlife, and other natural resources.

# 1. Introduction

## 1.1. Objectives

This document is a report to the Minnesota Department of Natural Resources (MNDNR) that provides a review of research conducted on wetland mapping methods for the Twin Cities Metropolitan Area (TCMA) in Minnesota. Given herein are recommendations for wetland mapping methods appropriate for the ongoing National Wetlands Inventory update in Minnesota. This document is provided to MNDNR by the University of Minnesota's Remote Sensing and Geospatial Analysis Lab (RSGAL) in partial fulfillment of a contractual agreement between the two parties. The structure of this report is as follows: 1) background information about wetlands and a review of relevant literature regarding wetland mapping, 2) detailed summaries of the research undertaken by RSGAL under this agreement, 3) Recommendations and a suggested protocol for wetland mapping in the TCMA.

## 1.2. Background

For regulatory purposes, wetlands are jointly defined by the U.S. Army Corps of Engineers (USACE) and the U.S. Environmental Protection Agency (EPA) as: "those areas that are inundated or saturated by surface or ground water at a frequency and duration to support, and under normal circumstances do support, a prevalence of vegetation typically adapted for life in saturated soil conditions" (Federal Register, 1982; Federal Register, 1980). Wetlands are valuable natural resources, as they play a crucial role in the ecology of a landscape. Wetlands function as a buffer to open water bodies and provide an important ecosystem functions by filtering nutrients and pollutants, storing floodwater and mitigating its effects on water bodies, and providing habitat to a variety of wildlife that have adapted to life in saturated environments. Wetlands also play a role in the global carbon cycle, acting as carbon sinks.

The United States has experienced significant wetland loss. In a 200 year period between colonization and the 1980's, the lower 48 states lost an estimated 53% of wetland acreage due to a variety of human activities such as agriculture, urbanization and development, and pollution (Dahl, 1990; Johnston, 1989). In Minnesota, over 50% of the state's 3.6 million ha of wetlands have been lost, mostly due to land drainage for agriculture in southern Minnesota and the Red River Valley. Urbanization causes small wetland area losses, but significantly alters a wetland's physical, biological, and chemical properties (Johnston, 1989). The loss of wetlands continues, but the rate of loss may be slowing (Dahl and Johnson, 1991). Accurate mapping of the spatial distribution of wetlands is important for understanding the effects of wetland loss (Baker, et al. 2006).

Mapping wetlands can be achieved through a variety of methodologies. Remote sensing has been used as a wetland mapping tool since the 1960's (Cowardin and Myers, 1974) but recent advances in remote sensing technologies may offer considerable increases in accuracy and cost-efficiency. The following presents a review of the current status and trends of the remote sensing of wetlands and examines the usefulness of a variety of data sources in enhancing the accuracy of wetland classification and mapping.

Wetland delineation and classification can be achieved using several methods. The most accurate method is field wetland delineation, where a wetland expert defines the boundary between wetland and upland using vegetative, soil, and hydrology field indicators. Field wetland delineation methods are described by the U.S. Army Corps of Engineers (1987). This method produces very accurate results but is also the most laborious and expensive. While required for regulated activities within wetlands, field delineation is often unnecessary for other wetland management uses.

Aerial photography is another data type that can be used to determine wetland boundaries. This type of inventory requires a trained interpreter to define wetland boundaries based on features distinguishable to the human eye on aerial photographs. Problems and inconsistencies may arise when multiple interpreters attempt to interpret the same photographs, as the accuracy of this method is determined by interpreter skill and experience (Baker, et al. 2006). A main disadvantage of aerial photograph interpretation is that inaccuracies are possible if the timing of the photography coincides with abnormal rainfall. (Ozesmi and Bauer, 2002). Harvey and Hill (2001) were able to achieve 90% accuracy when manually interpreting 14 land cover classes, including wetlands, in Australia using aerial photography (1:15,000 scale). The Minnesota Wetland Status and Trends Monitoring Program also relies on manual stereo-photo-interpretation and managed to achieve overall accuracies of 94% for wetland identification and 89% for wetland classification (Kloiber, 2010)

A third data type for mapping wetlands is remotely sensed satellite images. Use of satellite images has several advantages over aerial photography. Many satellites have sufficiently high temporal resolution to allow the acquisition of several images of the same location throughout a growing season. Satellites carrying sensors such as the Landsat Thematic Mapper (TM) allow for multispectral data collection at different wavelengths. The main disadvantage of satellite imagery is the lack of spatial resolution when compared to aerial photography. Harvey and Hill (2001) were unable to classify the same 14 land cover classes using satellite imagery that they were able to classify with aerial photography. An accuracy of 90% was achieved using satellite imagery only when the 14 classes were aggregated into three broader land cover classes.

### 1.2.1. Classification Methods

Several image classification methods have been developed and used historically to classify wetlands. No standard wetland classes are used, and target classes are often land-cover based and include types such as hardwood wetland, coniferous wetland, and herbaceous wetland. Henderson and Lewis (2008) point out inconsistencies in land cover definitions and, as an example, ask what percentage of canopy cover should be used to discriminate between open water and flooded forest. Specificity of wetland classes varies with classification goals and quality of input data.

The traditional and most commonly used classification method is an unsupervised classification of TM imagery (Ozesmi and Bauer, 2002; Sader et al., 1995). Although recognized as the least accurate method, unsupervised classification is often applied due to its elimination of time consuming training steps.

Hybrid classifications, described by Jensen (2005), combine unsupervised clusters with supervised training sets of known land cover. The training phase involves defining spectral signatures of known land cover and then incorporating those signatures into a classification model.

Another classification method uses TM derivatives to discriminate image texture. Vegetation indices such as the normalized difference vegetation index (NDVI), the TM Band 4:5 ratio, and the TM tasseled-cap model are used as textural information to further discriminate wetlands, particularly forested wetlands (Wright and Gallant, 2007; Hodgson et al., 1987).

Several researchers (Wright and Gallant, 2007; Sader et al., 1995) report a decrease in overall error when additional predictors are added to TM imagery classification. Wright and Gallant (2007) report an overall accuracy of 92.2% when discriminating palustrine wetlands from uplands. They further classified

the palustrine wetlands into five Cowardin types (aquatic bed, emergent, forested, scrub shrub, and unconsolidated shore) with an overall accuracy of 83%, consistent across 7 years of data. Sader et al. (1995) classified four land cover classes at two locations in Maine, and reported overall accuracies of 72% and 74% for unsupervised classification of TM imagery, 74% and 75% for unsupervised classification of the tasseled-cap transformation, and 81% and 78% for the hybrid classification (but with decreased producer's accuracy).

In addition to automated processes, visual interpretation of imagery can be a useful element in the classification process. Harvey and Hill (2001) reported that these semi-automated maps produced 9% more accurate results than completely automated approaches. Islam, et al. (2008) compared automated and semi-automated techniques and found that automated techniques using ETM+ imagery, Shuttle Radar Topography Mission (SRTM) data, and topography derivatives produced unacceptable results, while the use of semi-automated techniques produced 87% accuracy in distinguishing 15 wetland classes. However, the study was limited by the use of low resolution (90m) topographic data in automated classification. While shown to improve classification accuracy, the use of human interpreters introduces potential biases and inconsistencies into the classification process and certain training and methodological techniques must be utilized to prevent bias from affecting experimental results.

### 1.2.2. Multitemporal Data

Confusion between upland and wetland forested habitats is consistently reported when performing land cover classification based on one image (Lunetta and Balogh, 1999; Wang, 1998; Townsend and Walsh, 2001). Accuracy improvements in mapping of wetland habitats, especially forested wetlands, can be achieved using multiple dates of imagery collected throughout a growing season. This technique provides images of the same location with distinguishing features, such as canopy cover, biomass, and soil moisture, in various states.

Wolter et al. (1995) reported good results differentiating tree species in northwest Wisconsin using multitemporal data. Using five images, collected May through February in varying years, the author was able to achieve species level classification with an accuracy of 80.1%. Accuracy for Anderson Level II (hardwood, conifer, mixed) was 93.6%. Overall accuracy for 22 forest types was 83.2%. Successfully classified species included quaking aspen, sugar maple, northern red oak, northern pin oak, and tamarack (Wolter et al. 1995). Lunetta and Balogh (1999) compared single date to two date classification in wetland identification. Two dates of Landsat 5 TM data, leaf-on imagery to differentiate land cover types and spring leaf-off data to identify areas exhibiting wetland hydrology, produced an accuracy of 88% compared to 69% for single date. Wang (1998) reported an accuracy improvement in land cover classification from 51% with a single date image to 85% with multiple dates using JERS imagery. Likewise, Costa (2004) reported 93% accuracy for floodplain forest classification using JERS-1 and Radarsat-1 data collected throughout the wet season in the Amazon, with a drop in accuracy to 59% if only the one image was used during the first month of the dry season. However, Arzandeh and Wang (2003) reported that single date, single polarization, JERS imagery can be useful in delineating wetlands from non-wetlands, citing 88% accuracy in a study conducted in Ontario.

Townsend and Walsh (2001) combined multispectral and multitemporal techniques as they mapped wetland plant communities in North Carolina. Twenty-one forested communities were distinguished using Landsat TM data from three seasons (March-April, May-June, and July-August) in a single year. A hierarchical classification scheme was developed using feature sets from TM bands and their

combinations (NDVI, TM5/TM4). The authors report overall accuracy of 92.1% using discrete classification. When fuzzy class relationships were considered, accuracy increased to 96.6%.

### 1.2.3. Hyperspectral Data

Sensors such as the Airborne Visible/Infrared Imaging Spectrometer (AVIRIS) collect hyperspectral data in 224 spectral bands allowing for discrimination of individual species from images (Hirano et al. 2003).

Neuenschwander et al. (1998) used AVIRIS data to map coastal wetlands in Florida. The authors reported increased accuracy of identification of wetland vegetation (ranging from 85.0% to 93.5%, depending on classifier) when compared to using Landsat TM multispectral data. However, wetlands and uplands were separated based on biomass (NDVI). Willow swamps and forested swamps were included as uplands due to their high biomass. In addition, only 12 vegetative communities (upland and wetland) were distinguished, leading to high accuracy (Neuenschwander et al. 1998).

Hirano et al. (2003) mapped wetland vegetative communities in the Everglades National Park with hyperspectral AVIRIS data. Using only pure pixels from training sites established by manually interpreted CIR aerial photographs, the authors were able to distinguish 133 unique vegetative classes, which were compressed into 23 classes based on dominant vegetation. Accuracies varied between 40% and 100%, with an overall accuracy of 65.7%. Accuracy was limited by relatively poor spatial resolution (20m). Other reported problems with hyperspectral data are data volume and complex data pre-processing techniques (Hirano et al. 2003).

Becker et al. (2005) attempted to reduce hyperspectral data volume by isolating optimal spectral bands for use in mapping coastal wetland vegetation in the Great Lake region. The authors were able to isolate eight spectral bands that contained information enough to distinguish the regional vegetation. However, these spectral bands are specific to the coastal vegetative plant communities in the Great Lakes region. Becker et al. (2007) used seven of these eight spectral bands to classify wetland vegetation. Tests were also conducted to determine optimal spatial resolution. The greatest accuracy was reported with spatial resolution less than 2m. An overall accuracy of 86.3% was reported for the 7-band combination at under 2m resolution (Becker, et al. 2007).

### 1.2.4. Radar Imagery

Most of the focus of remote sensing of wetlands has been on sensors operating in the optical and infrared range of the electromagnetic spectrum, the limitations of which have been noted (Ozesmi and Bauer, 2002). Unlike optical sensors, radar sensors are unique in that they operate in the microwave portion of the electromagnetic spectrum and are insensitive to atmospheric conditions (e.g. cloud cover) and low light conditions, and can therefore offer more consistent multi-temporal images. Radar backscatter is sensitive to soil and vegetation moisture properties and can, to some degree, penetrate the forest canopy and provide sub-canopy vegetation and soil saturation information (Whitcomb et al., 2007; Henderson and Lewis, 2008). Because radar is sensitive to texture, techniques using interferometric analysis of radar data can identify changes in water levels down to the centimeter (Wdowinski, 2007).

Radar antennas can transmit radar waves of varying wavelengths. Common radar bands are C-band, L-band, and P-band, in order of increasing wavelength. Longer wavelengths tend to penetrate much farther into the forest canopy, thus providing a backscatter signal that conveys information about sub-canopy vegetation and moisture conditions (Whitcomb et al., 2007). Woody wetlands have high

backscatter and appear white, and are often confused with urban areas, while herbaceous wetlands have less backscatter and appear darker (Wdowinski, 2007). Wang (1995) used C-band, L-band, and P-band radar and found that high leaf area indices had an effect on C-band radar only, not L-band or P-band. Thus, L-band radar is significantly better at detecting flooded forests with intact canopy cover than C-band (Kasischke, 1997; Rosenqvist et al., 2004; Hess et al., 2003). Conversely, C-band radar is better at identifying herbaceous wetlands (Henderson and Lewis, 2008).

Radar waves can be sent and received at similar or dissimilar polarizations. Similar polarizations (HH, VV) are reported as useful in discriminating forested wetland/non-wetland by providing better image contrast than cross-polarization (HV), whereas cross-polarizations were preferable when distinguishing between forested swamps and herbaceous marshes (Hess et al., 1990; Hess et al., 1995).

Multiple studies report that a combination of C-band and L-band radar, as well as mixed polarizations, significantly increased accuracy of wetland/non-wetland discrimination and wetland vegetation classification (Hess et al., 1990; Hess et al., 1995; Dobson, 1995; Whitcomb et al., 2007; Henderson and Lewis, 2008). Henderson and Lewis (2008) wrote that cross-polarized imagery can be as valuable as single-polarized, multitemporal imagery. Studies also found that vegetation information is enhanced by using multitemporal and cross-polarized imagery and reported land cover accuracies above 90% when using SAR imagery (Kasischke, 1997; Dobson, 1995). Lozano-Garcia and Hoffer (1993) reported increased accuracy in land cover classification when they combined SIR-B data with Landsat TM data.

Whitcomb et al. (2007) used JERS to collect two seasons of L-band SAR imagery to produce a wetland map throughout the state of Alaska. Ancillary data sets including DEM (66m spatial resolution), map of open water, and latitude were included in the classification model. The Random Forests decision tree algorithm (Breiman, 2001) was used as a classifier. Nine wetland classes were aggregated which roughly correlated to the U.S. Fish and Wildlife Service's Circular 39 wetland classification (Shaw and Fredine, 2001). The authors reported accuracies ranging from 69.5% to 95%, depending on wetland class, with an overall accuracy of 89.5%. The NWI map for Alaska was used as test data set in the accuracy assessment. The authors suggest L-band in combination with C-band SAR will better distinguish between emergent wetland types (Whitcomb et al. 2007).

Henderson and Lewis (2008) provide the most recent review of usage of radar data to detect and classify wetlands. They reported that distinguishing wetlands and non-wetlands is consistently done with higher accuracy than discriminating wetland vegetative species. However, they noted that when mapping wetland species, most of the confusion is between wetland types and not between wetland and non-wetland vegetation. (Henderson and Lewis, 2008).

#### 1.2.5. Ancillary Data Sets

In addition to imagery, ancillary data sets may be used to derive valuable information. Digital elevation models (DEM) are most commonly used, from which can be derived a number of applicable datasets including slope, flow accumulation, and probability of soil wetness. Digital soil surveys such as the Soil Survey Geographic (SSURGO) product from the Natural Resources Conservation Service (NRCS) are also used to highlight areas of mapped hydric soils. GIS data sets are integrated into classification models using rule based classification or decision trees. Bolstad and Lillesand (1992) reported land-cover classification accuracy 16% higher (73-89%) for a GIS rule-based model incorporating TM imagery, soils, and terrain data than for traditional maximum likelihood TM imagery classification.

Creed et al. (2003) investigated optimal DEM spatial resolution and source while locating “cryptic wetlands” (i.e. “closed canopy wetlands with no distinct wetland-specific canopy species, as indicated by analysis of aerial photography and/or satellite images”) to determine their effects on dissolved organic carbon. LiDAR was found to be better at discriminating wetlands when compared to field based delineations ( $r^2 = 0.98$ ,  $p < 0.001$ ) than photogrammetric based DEMs. Comparisons of ability of automatically derived wetlands from scaled DEMs to manually derived wetlands were found to be significant up to 100m ( $p < 0.05$ ) with 5m, 10m, and 25m showing the greatest strength ( $r^2 = 0.98$ ,  $r^2 = 0.97$ ,  $r^2 = 0.99$ ;  $p < 0.001$ ) of correlation. Similarly, Thompson et al. (2001) attempted to predict the depth of the soil A-horizon using 10m and 30m DEMs and noted that, while differences in DEM resolution affect model coefficients and the DN values of terrain derivatives, each displayed similar capabilities in prediction A-horizon depth.

Murphy et al. (2007) compared vector based wetland polygons derived from manual aerial photography interpretation and wetlands areas in New Brunswick, Canada modeled using a depth-to-water index. The depth-to-water index uses the compound topographic index (CTI) and correlates the CTI value with depth to groundwater to determine wet areas. The authors report 51% - 67% of discrete wet areas are within the 0-10cm depth-to-groundwater class. The continuous (raster) depth-to-groundwater layer was derived from DEM with 70m grid spacing and used the D8 flow direction algorithm. The authors note that an improvement in DEM spatial resolution may increase accuracy, and that smaller (<1ha) wetlands were likely missed. Authors also point out that raised bogs characterized by a higher elevation due to accumulation of peat are sources of error when using derivations of elevation data to determine likelihood of saturation (Murphy et al., 2007).

Hogg and Todd (2007) also used DEM data and compared the effectiveness of several delineation methods in distinguishing several wetland types (marsh, swamp, bog, fen, etc). Many DEM derivations were calculated, and the CTI (using the D-infinity algorithm) and the positive balance hydraulic slope (PMNB) were determined to be the best at distinguishing wetlands and threshold values were established for input into a classification and regression tree (CART). The authors compared several statistical methods and found the CART to be the most accurate, reporting results of 90% calibration accuracy and 84% validation accuracy. The authors stress the usefulness of terrain data above optical data because its delineations of wetland boundaries are easily repeatable; however, unlike optical data it lacks sensitive wetland mapping triggers such as observable moisture (Hogg and Todd, 2007; Lang and McCarty, 2009)

Baker et al. (2006) used Landsat ETM+ data from May and September to classify land cover and wetland/riparian systems in Montana. Multitemporal images were used only to assess changing hydrology throughout the growing season and were not used to classify vegetation. Ancillary data included a 30m DEM and hydric soils maps. Authors compared accuracy of Classification Tree Analysis (CTA) and Stochastic Gradient Boosting (SGB) classifiers and reported an overall accuracy of 73.1% with the CTA and 86.0% with the SGB (Baker et al. 2006).

Li and Chen (2005) present an easily comparable analysis between assessment methods. The authors used multiple dates of DEM, Landsat ETM+, as well as Radarsat-1/SAR data and a rule-based classification method to distinguish between bogs, fens, swamps, marshes, and shallow water habitats in eastern Canada. Authors report accuracy of 71% to 92%, depending on wetland type, compared to traditional methods using ETM+ alone (24-89%) and ETM+ and SAR in combination (78-85%). The rule-based method is presented in a clear, stepwise manner. The authors also report that the addition of radar data to optical data helped delineate shrub/tree wetlands from shrub/forest upland, but it may

have had a negative effect on the overall land cover classification accuracy from the introduction of speckle and noise.

In summary, while numerous approaches have been used in wetland mapping, there is no universally applicable method. The choice of data source and mapping method is governed by the types of wetlands being mapped and the desired level of thematic detail. The following sections of this document describe mapping method experiments conducted using Minnesota's wetlands.

## **2. Methods/Results**

### **2.1. Wetland Mapping using Terrain Indices**

#### **2.1.1. Terrain Indices Introduction**

Recent technological advances have allowed the acquisition of elevation data at higher resolutions than ever before. With this new data (i.e. LIDAR) comes opportunities to derive more accurate topographic attributes for landscapes. A Digital Elevation Model (DEM) provides the base data to calculate catchment area, upslope area, slope, aspect, and secondary information such as terrain indices. Terrain indices such as the Compound Topographic Index (CTI) and Slope Cost-Distance Index (SCDI) are indicators of the expected "wetness" of an area based on the amount and direction of surface water flow (Blyth et al., 2004; Guntner et al., 2004; Moore et al., 1991). Such terrain indices can identify parts of the landscape where sufficient wetness could be present to allow the formation of wetlands. Therefore, topographic information can assist in mapping depressional and flat areas that may contain wetlands. This information can provide more accurate and timely wetland maps than the current Minnesota National Wetlands Inventory (NWI), which is of limited utility because of the scale of the aerial photos used to do the mapping and the significant changes that have occurred since the maps were created. As a consequence, there is a great need to update wetlands maps with more accurate boundaries, better type classifications, and improved delineation of smaller wetlands.

In this study, four approaches were evaluated to determine how topographic data can assist with wetland mapping in Minnesota. The first and second approaches involved assessing the effectiveness of two topographic indices: CTI and SCDI derived from a 3m resolution DEM. The third approach evaluated the resolution sensitivity of the CTI and SCDI created from 9 m, 12 m, 24 m, and 33 m LiDAR DEMs; the 10 m National Elevation Data; and a 30 m USGS DEM. The fourth approach evaluated combining CTI, aerial imagery, and soil data to map wetlands. The goal of this evaluation is to identify methods to increase the accuracy and decrease the cost of mapping wetlands.

#### **2.1.2. Terrain Indices Methods**

The study area for this project was the city of Chanhassen in Carver County, Minnesota. This area was chosen because it represents the range of Minnesota Metro area wetland types and because high quality field reference data was available for this area. Spatial data development, manipulation, and analysis were completed using ESRI's ArcGIS 9.3 with the Spatial Analyst, 3-D Analyst, and TauDEM (Terrain Analysis Using Digital Elevation Models) tools. All data sets were projected to UTM Zone 15N, NAD83. The following data sets were used in this study:

- I. Hydrographic Datasets

- a. DNR 24K streams
  - b. DNR 24K lakes
  - c. USFWS National Wetland Inventory
  - d. City of Chanhassen Wetland Inventory (August 2006, data collected using GPS equipment in 2004-2005)
- II. Topographic Datasets
- a. LIDAR elevation data: 3m DEM
  - b. NED elevation data: 10 m DEM
  - c. USGS elevation data: 30 m DEM
- III. Aerial Photography
- a. U.S. Department of Agriculture's National Agriculture Imagery Program (NAIP), 1-meter resolution, 2008 digital images with four bands: red, green, blue, color-infrared (CIR)
- IV. Soil Survey Geographic (SSURGO) Database
- a. Hydric Soils
  - b. Very poorly drained

#### ***2.1.2.1. Approach 1 – Compound Topographic Index (CTI)***

The CTI is an indicator of potential saturated and unsaturated areas within a catchment area (e.g. a watershed). The CTI is the natural log (ln) of the ratio of the Specific Catchment Area (As) expressed as m<sup>2</sup> per unit width orthogonal to the flow direction divided by the tangent of the slope ( $\beta$ ). Thus,  $CTI = \ln [(As) / (\tan (\beta))]$ . For comparison purposes, two types of CTI were created for the city of Chanhassen; one was created using the D-8 flow modeling approach and the other one using the D-Infinity (D-inf) flow modeling approach.

Prior to calculating the CTIs the 3m LiDAR, 10 m NED and 30 m USGS DEM were clipped to the boundary of the city of Chanhassen. The following steps were performed to create the two types of CTI:

##### *Step 1 - DEM Reconditioning and Fill Sinks*

Elevation irregularities (e.g. erroneous sinks and peaks) that could interfere with the correct hydrologic flow were removed using the ArcHydro and TauDEM tools. A hydrology layer was used to burn in streams to the DEM. Road berm dams were manually corrected in situations where they appeared to affect water flow.

##### *Step 2 - Flow Direction*

After removing elevation irregularities, the next step was to create a flow direction grid for each DEM, one using the D-8 method and the other using the D- inf method. The D8 method is limited to one of eight directions and assumes that flow is limited to one cardinal direction and one of two specific widths, routing the flow from one cell to a single neighbor. This has the effect of representing convergent flow (multiple cells flowing to a single cell), while stopping the representation of divergent flow (a single cell flowing to multiple cells). In the real world, flow most likely diverges and converges at different places and periods.

The D-inf algorithm assigns a flow direction based on the steepest slope on a triangular facet by constructing facet from the DEM (Tarboton 1997, Douglas 1986). This method is capable of creating a multi-directional flow, representing a divergent flow. D-inf offers an alternative method of calculating slopes, flow directions, and contributing area through the accumulation of converging and diverging flow directions.

### *Step 3 - Contributing Area*

A watershed is the upslope area contributing flow to a given location. This area is also referred sometimes as a basin, catchment, or contributing area. A contributing area grid was delineated for each algorithm method. In the ArcHydro tool this was done using the D-8 flow direction grid. Alternatively, in TauDEM tool the D-inf algorithm approach was taken to calculate the contributing area. This gives a contributing area grid evaluated by accumulating the area or weight loading upslope of each location.

### *Step 4 - Specific Catchment Area (As)*

Specific Catchment Area is a raster grid representing upslope contributing area. A specific catchment area grid was created for each approach. This is measured in specific catchment area units, i.e. area per unit contour width, using grid cell as the unit width and grid cell size squared as grid cell area.

### *Step 5 - Slope Grid*

The slope grid is a raster grid representing change in elevation between adjacent pixels. A slope grid was derived directly from the DEM and a minimum value of 0.0001 was imposed on the resulting calculated slope to avoid division by zero for future CTI calculations. This was created using the raster calculator from Spatial Analyst extension: Slope grid + 0.001

### *Step 6 - Map Algebra – CTI Calculation*

Once all the required grids were created (Specific catchment area and Slope), the raster calculator from Spatial Analyst extension was used to calculate the CTI using the CTI equation:  $CTI: \ln [(As) / (\tan (\beta))]$ , where  $As$  is the specific catchment area expressed as  $m^2$  per unit width orthogonal to the flow direction and  $\beta$  is the tangent of the slope in Radians.

### *Step 7 - Low Pass Filter Operation*

A low pass filter was used for each type of CTI created to reduce the significance of anomalous cells.

### **2.1.2.2. Approach 2 – Slope Cost-Distance Index (SCDI)**

The SCDI calculates for each cell the least accumulative cost to specified location. This is a function of the drainage line and slope grid. The first five steps of the computation of the SCDI are the same as those for the CTI. The following additional steps were performed.

### *Step 6 - Stream Definition*

The stream definition function from ArcHydro was used to extract cells with flow accumulation grid values above a certain threshold. This threshold was defined as a number of cells, for this study a 1% area threshold was used.

#### *Step 7 - Stream Segmentation*

The stream segmentation function from ArcHydro was used to break up the streams into head segments and joint segments.

#### *Step 8 - Drainage Line Processing*

This function from ArcHydro was used to convert the stream segmentation grid into a vector layer.

#### *Step 9 - Spatial Analyst Calculation to obtain the Slope Cost-Distance Index*

The Cost-Distance function from Spatial Analyst tool was used to create the SCDI. This function finds the path of least resistance in which water is assumed to flow. The drainage network vector layer (Drainage Line) was used as an input direction and the slope grid was used as the cost grid. Since, the SCDI is a comparative function rather than a calculated function like the CTI, absolute values of slope do not matter and degrees or percentage are acceptable as units.

### ***2.1.2.3. Approach 3 – CTI & SCDI Resolution Sensitivity***

To assess the resolution sensitivity of the CTI & SCDI the 3 m LiDAR DEM was degraded to 9, 12, 24, and 33 meters. This degradation process was done using the degrade tool from ERDAS IMAGE 9.3. This tool uses an average pixel method to make up the new larger pixels. Once all the new DEMs were created, the next step was to proceed with the creation and evaluation of the CTI & SCDI for each DEM.

### ***2.1.2.4. Approach 4 – Use of CTI, NDVI & Soils Data to Identify Wetlands***

Three data sets were used to develop this approach. The first data set was the CTI layer previously explained, the second was the soil layer obtained from Soil Survey Geographic (SSURGO) extracting only the hydric and very poorly drained soils were used, and the third was the NAIP imagery 2008.

For the NAIP imagery, a Normalized Difference Vegetation Index (NDVI) was calculated,  $NDVI = (NIR - RED) / (NIR + RED)$ , where NIR represent the near infrared band and RED represent the red band. This is a numerical indicator of the amount of live green vegetation in an image pixel. The purpose of the NDVI in this analysis was to exclude areas that are topographically suitable for wetlands but contain non-vegetated or impervious cover. A threshold of less or equal to 0.18 NDVI was used. Anything less or equal to this value was considered to be impervious, and anything greater than this value was considered to be vegetation. The NDVI was calculated from the NAIP imagery (2008), using band 4 = NIR and band 1 = Red. A hydrology layer was used to ensure that open water such as lakes and rivers was not removed due to its low NDVI.

#### *Boolean and Arithmetic Steps*

Once the CTI, NDVI, and soil layer were ready, boolean and arithmetic steps were used to determine whether each pixel was considered to be wetland or upland. The following steps were performed to combine these three layers.

- 1) **Reclassification of CTI values:** Based on threshold values, the CTI was reclassified either as wet represented by number 1 or dry represented by number 0. Any value greater or equal than the mean + ½ standard deviation of the CTI values was reclassified as wet (1), the rest was considered dry (0).  
Output = *CTI\_R* (new CTI reclassified layer)
  
- 2) **Reclassification of NDVI values**  
Based on threshold values the NDVI was reclassified either as vegetated or non-vegetated. In this model the number 0 was assigned to all the values representing non-vegetated, which in this model represented upland. Threshold  $\leq 0.18$  = Impervious (0); Output = *NDVI\_R* (new NDVI reclassified layer)
  
- 3) **Reclassification of Soil values**  
For the reclassification of soil values the Hydric soil + Very Poorly Drained soils were converted from vector to raster, reclassified as wet, and assigned the value of 1, representing wetness.  
Output = *Soil\_R* (new Soil reclassified layer)
  
- 4) **Raster Calculator:** this tool was used to create the first combination of NDVI and CTI in one layer. The following equation was used for this calculation:  
Equation 1:  $(NDVI\_R) \text{ AND}^* (CTI\_R) = Input\_A$   
  
\* CAND is a logical tool from ArcGIS that performs a Combinatorial And operation on the cell values of two input rasters.
  
- 5) **Raster Calculator:** The second equation was the combination of the Input\_A ( NDVI + CTI) and the soil layer  
**Equation 2**  
 $(Input\_A) \text{ AND} (Soil\_R) = Input\_B$
  
- 6) **Reclassification of Input\_B grid:** This was the final step performed to reclassify the values from input\_B, either as wet =1 or dry =0, which at the end the number 1 is translated as the potential pixel wetland value.  
1 = wet  
0 = Dry

#### 2.1.2.5. Accuracy Assessment of the Four Approaches

A pixel by pixel accuracy assessment was carried out to evaluate the four approaches taken for the use of topographic data in identifying potential wetlands. This was done by comparing the results from each of the four approaches to a “boots-on-the-ground” wetland delineation for Chanhassen, MN. An error matrix which compares the reference class values to the assigned class values in a  $c \times c$  matrix, where  $c$  is the number of classes was generated. In addition, an error matrix was created to provide summarize information on classification accuracy.

The following statistics were computed:

- Percent overall accuracy
- Error matrix
- User’s accuracy (considers commission errors)

- Producer's accuracy (considers omission errors)

### 2.1.3. Terrain Indices Results

#### 2.1.3.1. Study Area

Figures 1 and 2 show the city of Chanhassen geographic location and elevation data. The city of Chanhassen is located in the southwest metropolitan area of the Twin Cities of Minneapolis and St. Paul. While the bulk of Chanhassen is in Carver County, it also extends into Hennepin County. The City is approximately 23 square miles.

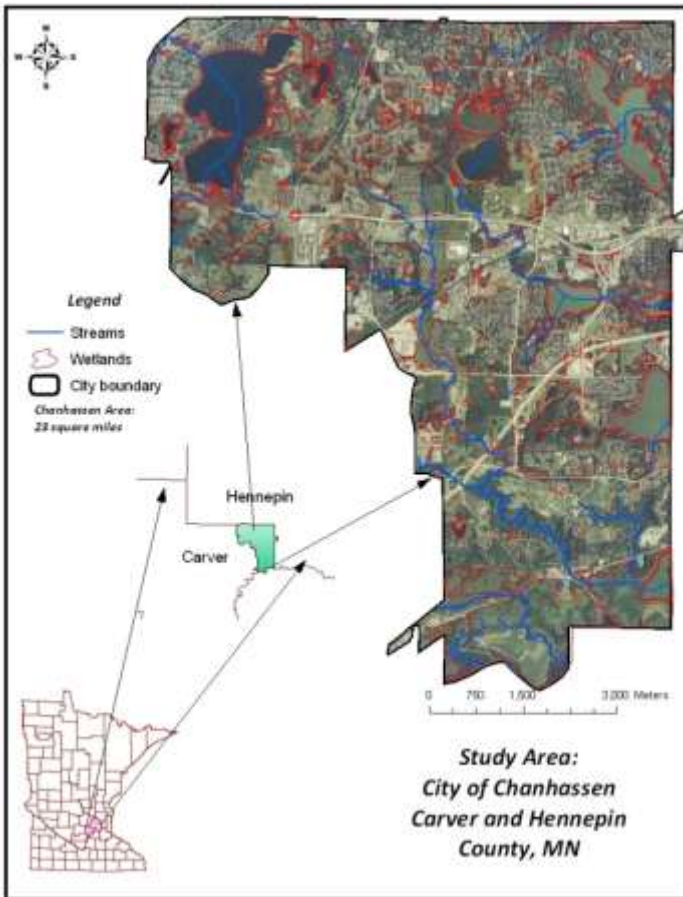


Figure 1. Location of the study area.

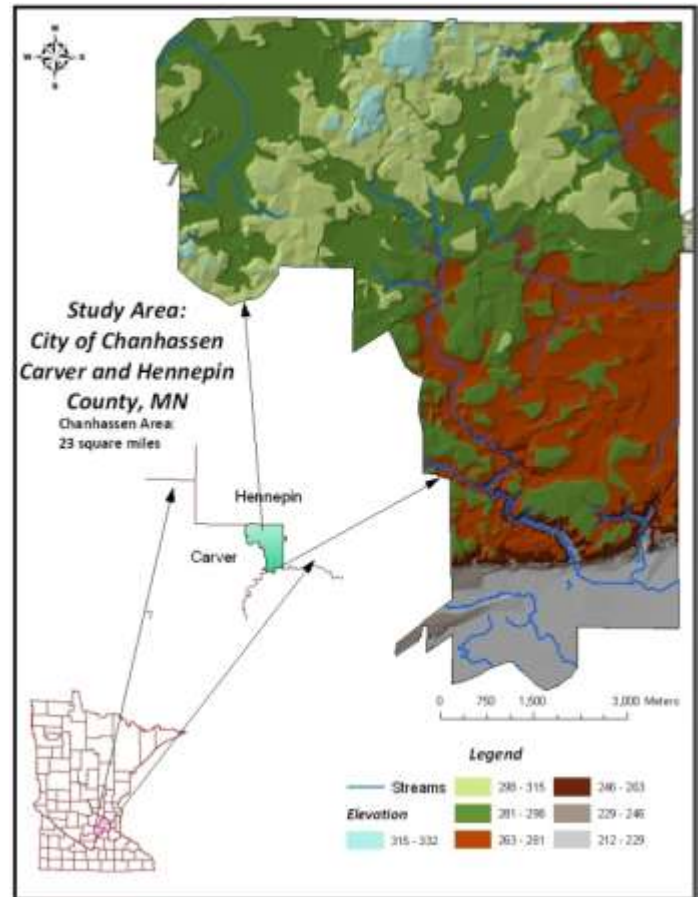


Figure 2. Elevation map of the study area.

#### 2.1.3.2. Wetland Sizes in the Study Area

Table 1 shows the different size of wetlands existing in the city of Chanhassen. More than 60% of its wetlands are less than 1 acre. Only 7.7% are greater than 10 acres.

Table 1. Wetland size for the city of Chanhassen.

Acre Size	# of Wetlands	% of study area	Cumulative %
0.1 - 0.5	202	46.9	61.7
0.5 - 1	64	14.8	
1 - 2	61	14.2	75.9
2 - 3	27	6.3	
3 - 6	24	5.6	92.3
6 - 10	20	4.6	
10 - 25	14	3.2	
25 - 50	9	2.1	
50 - 70	2	0.5	
70 - 100	2	0.5	
100 - 150	3	0.7	
> = 150	3	0.7	
Total	431	100	

**2.1.3.3. Comparison between the USFWS National Wetland Inventory (NWI) and the City of Chanhassen Wetland Inventory**

Figures 3 and 4 show some of the problems of the USFWS NWI. Some of the problems represented in these figures are the significant changes that have occurred due to urban development in five years.

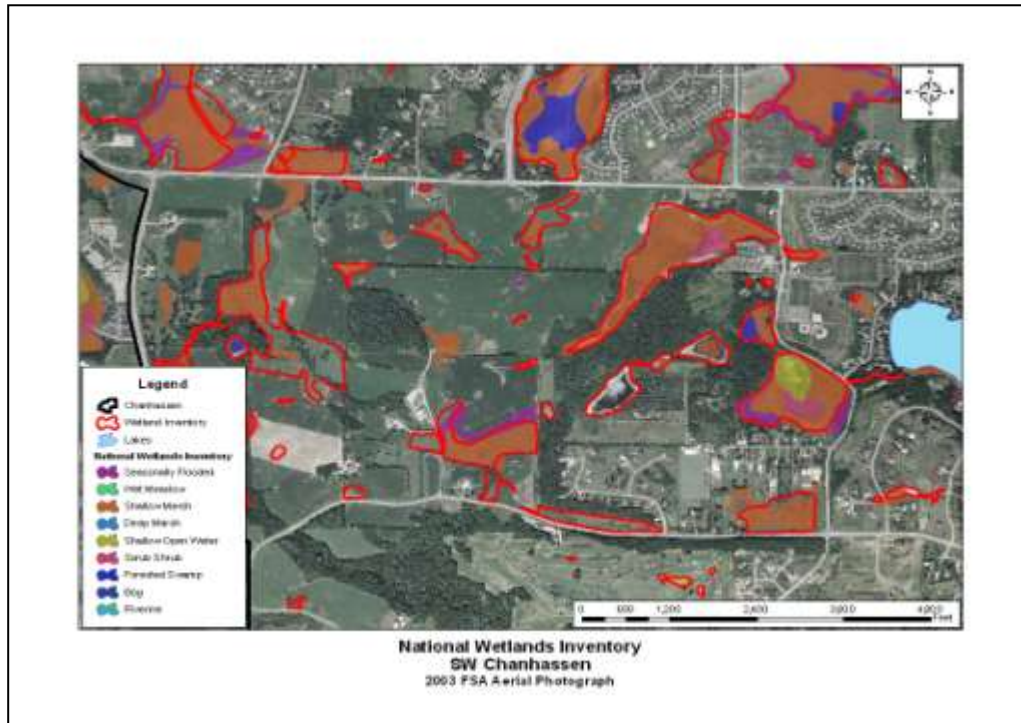


Figure 3. Comparison between the USFWS NWI and the City of Chanhassen Wetland Inventory on 2003 NAIP images.

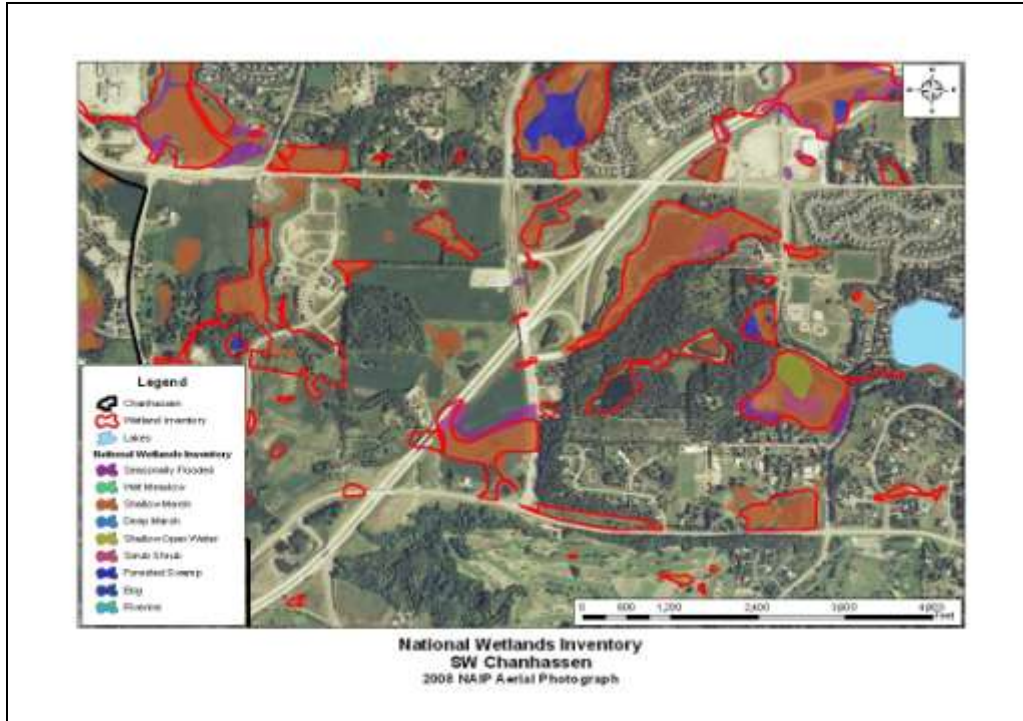


Figure 4. Comparison between the USFWS NWI and the City of Chanhassen Wetland Inventory on 2008 NAIP images.

#### 2.1.3.4. Accuracy Assessment results for Approach 1 (CTI) and Approach 3 Resolution Sensitivity (CTI)

An accuracy assessment tool was used in ArcGIS 9.3 to generate an accuracy assessment report for each resolution. Table 2 shows the results of this evaluation. This table shows clearly that the best resolution for identifying potential wetlands was 24 m with the highest producer accuracy percentage compared to the 10 m NED and 30 m USGS DEM.

It is notable that the highest errors of omission (omitting wetlands) were for the CTI derived from the NED and USGS DEM (Figure 5). At the same type the LiDAR data presented some problems due to the amount of details in the 3 m resolution (Figure 6), causing that resolution to have the highest percentage of error of commission (classifying pixels as wet when they are not) compared to the rest of the derived resolutions.

Table 2. Accuracy assessment results for CTI using the D-inf algorithm and created for the 3, 9, 10, 12, 24, 30, 33 m resolution.

CTI – D-infinity algorithm			
CTI from DEM	Overall Accuracy	Users Accuracy	Producers Accuracy
3m	86	68	85
9m	88	72	88
12m	89	73	88
24m	90	76	87
33m	90	77	86
10 m NED	88	76	77
30 m (USGS)	84	74	69

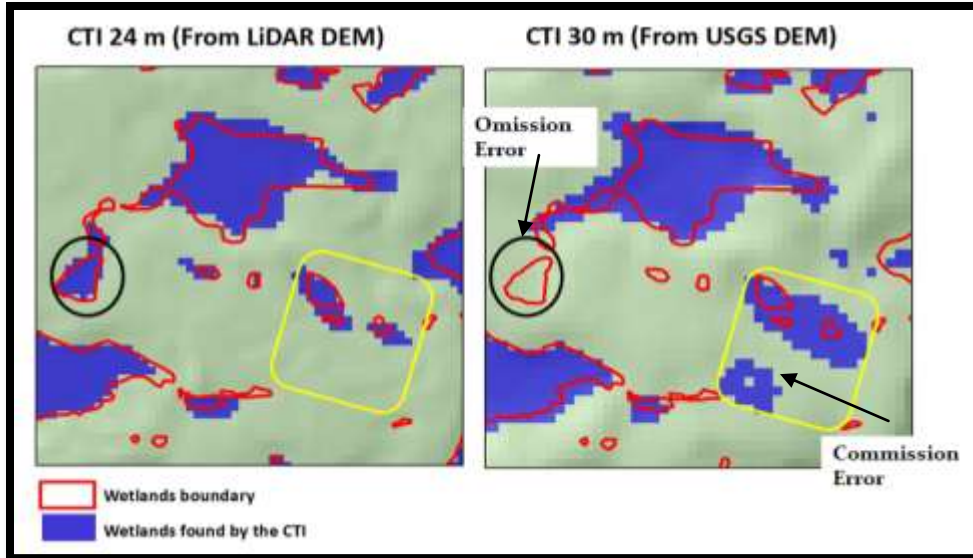


Figure 5. Comparisons between the CTI 24 m derived from LiDAR DEM & the CTI 30 m derived from the USGS DEM.

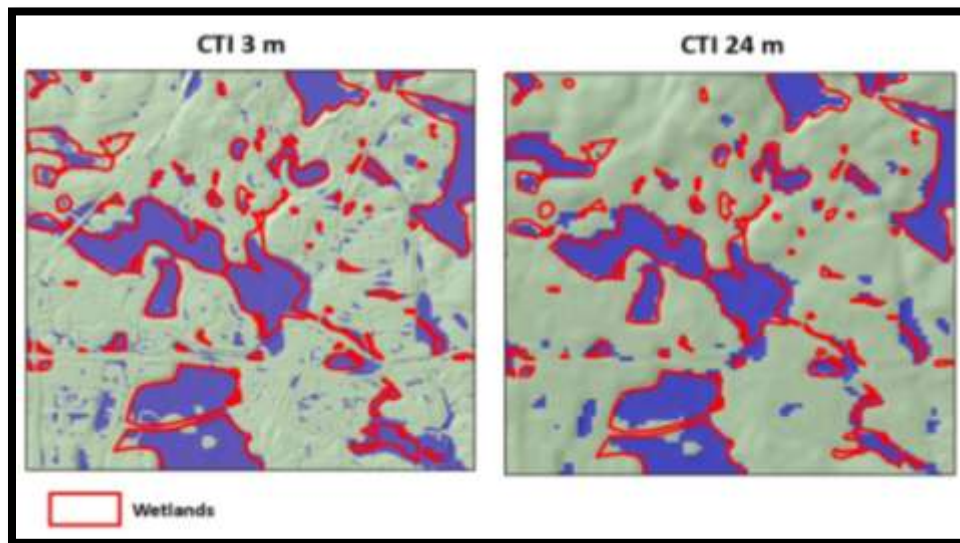


Figure 6. Comparisons between the CTI 3 m & CTI 24 m derived from LiDAR DEM.

### 2.1.3.5. Comparison between D-8 vs. D-infinity

The D-8 and D-infinity (D-inf) approaches were evaluated and the CTI was created for each method. Results (Table 3) indicate that both approaches have their benefits and disadvantages. Table 3 shows that the CTI derived from the D-inf approach has the highest producer's accuracy, which means the errors of omission are lower than those for the D-8 method. On the other hand the CTI derived from the D-8 approach has the highest user's accuracy, which means the errors of commission are less compared to the other approach. Figures 7 and 8 show the D-8 and D-inf CTI layers.

Table 3. Comparison between D-inf and D-8 algorithm method

CTI	DEM	Overall Accuracy	Users Accuracy	Producers Accuracy
CTI - D-Inf	24m	90	76	87
CTI- D-8	24m	90	83	77

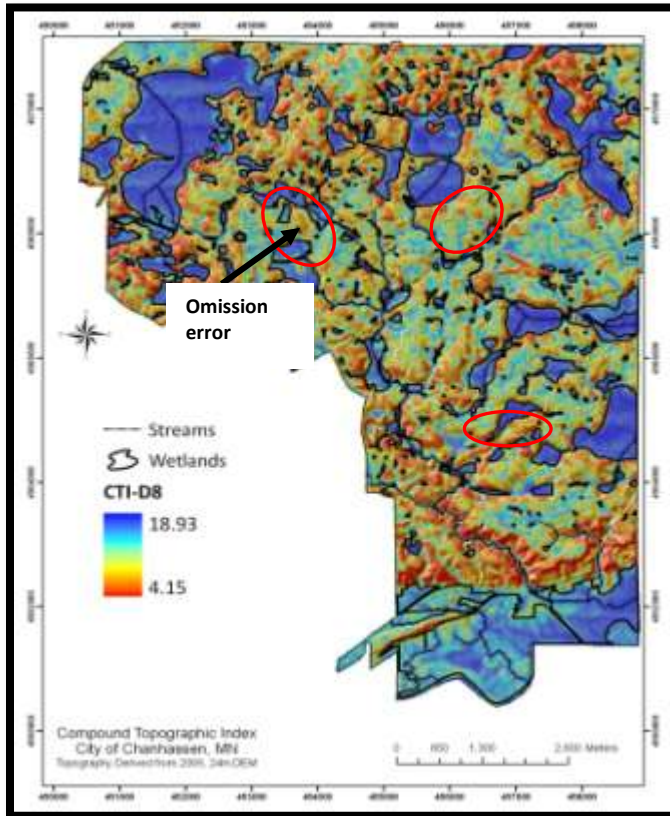


Figure 7. CTI 24 m derived from LiDAR DEM using the D-8 algorithm

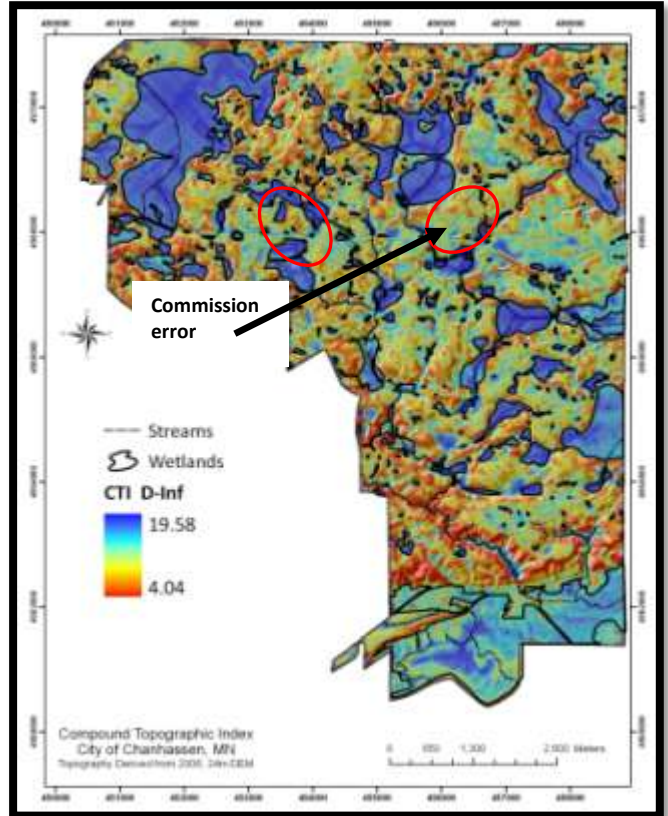


Figure 8. CTI 24 m derived from LiDAR DEM using the D-inf algorithm

### 2.1.3.6. Accuracy Assessment results for Approach 2 (SCDI) and Approach 3 Resolution Sensitivity (SCDI)

Table 4 shows the results for the accuracy totals for the SCDI. This table shows clearly that the highest overall accuracy and producer accuracy was for the SCDI derived from the 24m DEM. This indicates that resolution affects the efficiency of this index to identify potential wetlands (Figure 9).

Table 4. Accuracy assessment results for SCDI using the D-8 algorithm, created for the 3, 9, 12, 24, 33 m resolution.

SCDI			
DEM	Overall Accuracy	Users Accuracy	Producers Accuracy
3m	87	79	72
9m	88	77	81
12m	88	77	81
24m	88	76	82
33m	87	75	79

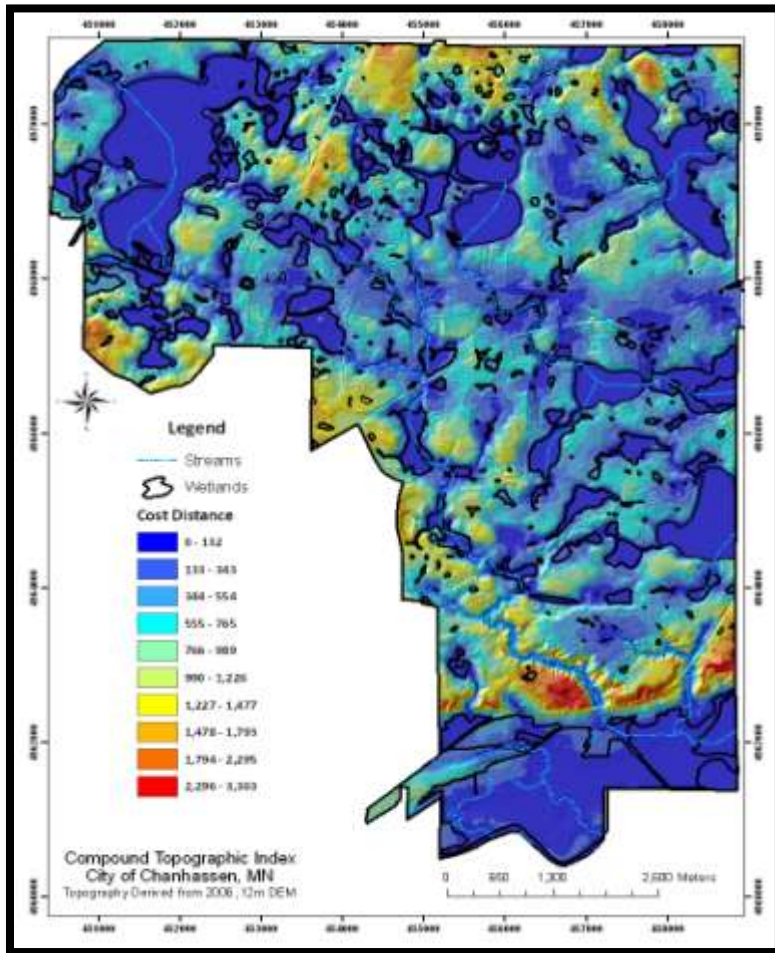


Figure 9. SCDI 24 m derived from LiDAR DEM using the D-8 algorithm

**2.1.3.7. Results and accuracy assessment percentages for approach # 4 Combination of CTI, NDVI & Soil**

Including the NDVI in the model improved the results by eliminating flat impervious surfaces, such as parking lots, from the wetland class predicted by the CTI alone (Figure 10 and 11). The NDVI values for image pixels containing buildings are low in Figure 10. In the NDVI shown in Figure 11, these areas are indicated as non-vegetated, and so are removed from consideration as potential wetlands, even if they are topographically suited to be wet.

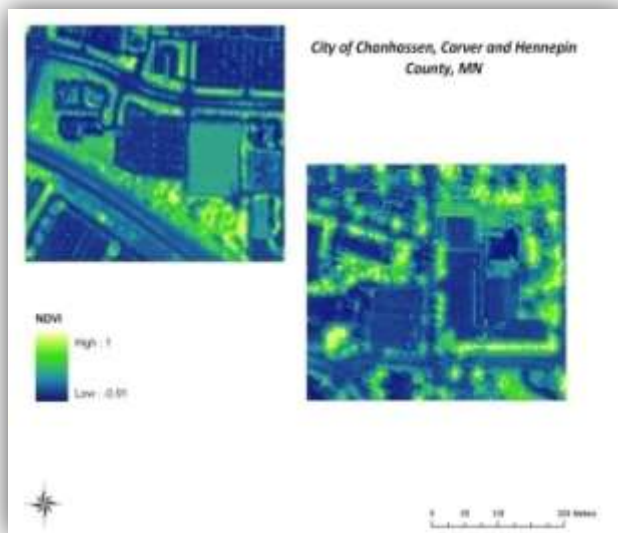


Figure 10. Low (wet) CTI values in impervious surface areas.



Figure 11. Areas removed from consideration as wetlands due to NDVI values.

Since the 24 m DEM provided the highest accuracy, for the combined model only the 24 m DEM was used. Table 5 shows the results of the inclusion of soil and NDVI data. The user’s accuracy increased sharply when these data were added to the model. Figure 12 shows a graphical depiction of the benefits of using soils and NDVI data in wetlands mapping.

Table 5. Accuracy assessment results for the combination of CTI, NDVI & Soil for 24 m

Acres	Combinations	DEM	%Overall Accuracy	% User Accuracy	% Producer Accuracy
0.1 to 788	CTI	24m	90	76	87
0.1 to 788	CTI + NDVI + Soils	24m	92	82	86
>= to 1	CTI + NDVI + Soils	24m	92	82	89

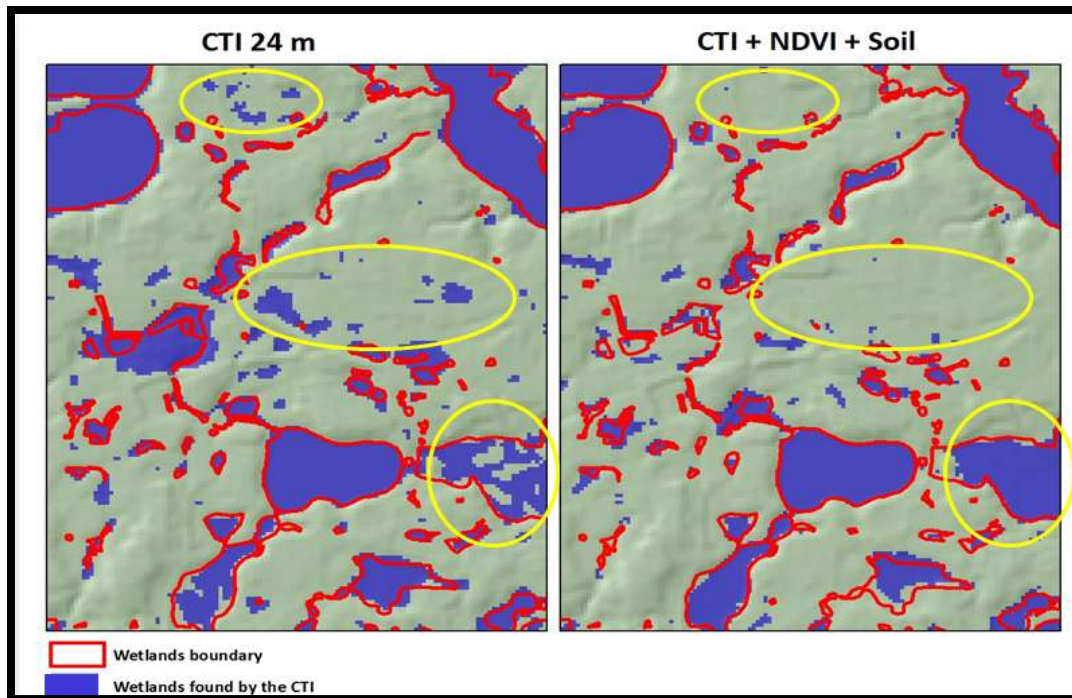


Figure 12. Comparison between CTI alone and the combination of the three layers.

#### 2.1.4. Terrain Indices Discussion

A comparison of the two methods (D-8 and D-inf) show that both methods have similar overall accuracy results, nevertheless, there is a slight difference between the producer's and user's accuracy estimates for both methods.

The CTI/D-inf/LiDAR derived map is significantly more accurate in producer's accuracy (87%) compared to the CTI/D-8/LiDAR derived map (77 % producer's accuracy), and has a lower rate of wetland omissions (Table 3, Figure 8). On the other hand, the CTI/D-8/LiDAR derived map had a much lower 17% commission error and higher user's accuracy (83%) relative to the CTI/D-inf/LiDAR derived map (76% user's accuracy and 24% commission error), which means that this method is able to classify more pixels correctly as wetland compared to the D-inf. (Table 3, Figure 7).

There are a few general issues that are important to consider when using these methods. The TauDEM tool/D-inf method will only work with DEM grids smaller than 7000 \* 7000 cells (approximately 100-miles by 100-miles with a 24-m resolution DEM) and it requires Windows 2000 or higher, plus ArcGIS 8.2 or higher version to run this tool. Alternatively, ArcHydro tool/D-8 method can work with any DEM grid size and works with any type of ArcGIS desktop version. Both tools are available to be run with an ArcGIS desktop version, with the only limitation for TauDEM tool regarding the DEM grid size.

We observed classification accuracies for the SCD/LiDAR derived maps (Table 4) that were similar to the CTI/LiDAR derived maps (Table 2). Omission errors were lower in the CTI/LiDAR derived maps relative to the other index. Thus, CTI surpasses SCD almost in every aspect such as better delineation boundaries and less wetlands omission (Figures 8, 9).

The SCD/LiDAR derived map also has some limitations such as the error of misclassifying many pixels as wet because of the method used to create this index. This index calculates water accumulation based in finding the path of least resistance in which water is assumed to flow based on a drainage line. This principle limits the potential of finding wetlands that are far away of a drainage line or streams. Thus, this may not be a good index to use in areas with a few streams or drainage lines.

LiDAR data proved useful in increasing classification accuracy in our study area, primarily in identifying wetland/upland types, local low areas in the terrain based on elevation differences and flow direction. (Figures 5, 6). For example the CTI/USGS derived map show higher errors of omission (Table 2, Figure 5) compared to the CTI/LiDAR derived maps. Simply replacing the USGS 30-meter DEM with a 24-m DEM derived from LiDAR significantly improved wetland identification from 84% overall accuracy to 90% overall accuracy .

High resolution images such as NAIP are useful for mapping wetlands, and are actually better than the aerial photographs used to create the original NWI. While mapping accuracies using terrain indices alone were reasonable (84 to 92%), accuracies improved when the CTI/LiDAR map was combined with the high resolution imagery (NDVI) and soil data (Table 5, Figure 13). Our result shows that errors of commissions were significantly reduced from 24% (CTI/LiDAR) to 18% (combination of CTI/LiDAR, NDVI, soils), while not significantly increasing omission error rates. This combination of data types better performance than using LiDAR data alone.

Based on these observations, we can infer that LiDAR data may help identify terrain features such as steep local gradients, the edges of flat areas, and delineation of a more accurate wetland/upland boundary. However, these terrain indexes may work better in conjunction with spectral data and other type of ancillary data such as soils type. Therefore, it is necessary to explore other types of LiDAR/ancillary data combinations to continue to improve accuracy in wetland boundary delineations. One possible option is the use of other algorithms such as decision trees or models that could automate the process of combining several layers (CTI, NDVI, soils) instead of the use of Boolean steps to create this type of combinations as was done in this study.

In terms of wide scale use, this method would be difficult to scale up to the entire state. Processing a state-wide DEM to compute CTI may present a significant computing challenge. Possible solutions include using migrating the processing to a supercomputer or tiling the study area.

### **2.1.5. Terrain Indices Conclusions**

- CTI does better job than SCDI in finding potential wetlands.
- DEM resolution is an important factor affecting the potential use for mapping wetlands, but quality of the source data can also have a significant effect on results.
- There is a great need to obtain higher resolution elevation data such as LiDAR, because this type of data may offer better results in the development of terrain indices and hence the automation for finding wetlands using topographic data. In this study a LiDAR DEM outperforms a 30 m (USGS) in overall accuracy

- From the four approaches evaluated in this study the best approach to use for finding wetlands using a GIS approach is the combination of CTI + Soil +NDVI. This approach does better job than terrain indices alone.
- The use of topographic data in combination with other ancillary data allows for automated delineation of wetlands in a more accurate way.

## 2.2. Wetland Mapping using Object Oriented Algorithms

### 2.2.1. Introduction to Object-Oriented Classification

Supervised and unsupervised classification approaches in remote sensing assign each pixel to a known information class or cluster class without regard to location or spatial relationships. These per-pixel classifiers have no way to account for spatial patterns in the classes, nor any way to examine adjacent pixels in the image for similarities. In contrast, object-oriented classifications first group pixels into clusters of homogeneous pixels based on set maximum heterogeneity thresholds, and then classify those clusters based on their aggregated statistics rather than individual pixels. Also, because pixels are grouped prior to any analysis, object-oriented classifications help reduce image speckle (Hess et al, 2003), decrease the effects of shadows within an image, and eliminate the need for post-classification smoothing, since the use of image objects prevents the “salt and pepper” effect of per-pixel classifications.

Wetland vegetation is highly heterogeneous, both within a single wetland and among wetland classes, making discrimination between wetland classes difficult (Grenier et al, 2007; Fournier et al, 2007; Bruzzone and Carlin, 2006). In addition, wetlands have complex spatial arrangements often characterized by alternating patches of open water and vegetation interspersed throughout the wetland, which complicates the delineation of wetland patches as a contiguous whole. Because object-oriented methods are able to connect neighboring pixels, they are also the better choice for creating ecology-based classification rules and combining the ancillary environmental datasets that are best able to identify wetlands (Fournier et al, 2007; Grenier et al, 2007).

When using high spatial resolution imagery, as required by the Federal Geographic Data Commission (FGDC) wetland mapping standard, the spectral variability within each wetland class increases at the expense of between class variability (Bruzzone and Carlin, 2006; FGDC, 2008). Therefore, object-oriented methods are advantageous when attempting to identify and classify wetlands in accordance with the FGDC standard. For example, a pixel-based classification scheme identifying adjacent open water and forest wetland pixels would likely separate the two into separate classes due to their spectral differences. This is the most significant limitation of the pixel-based classifier’s is its inability to view similarity and distance between pixels. For wetlands exhibiting high spatial patchiness or heterogeneity, accurate delineation and classification of the wetland as a whole depends on the ability to group adjacent pixels and to represent spectrally different patches within a single wetland polygon.

Object-oriented classifications require two steps. First, image segmentation, the prerequisite to object-oriented classification, divides an image into segments or pixel objects by merging adjacent pixels into statistically homogeneous groups (Fournier et al, 2007; Repaka et al, 2004). Variation within a segment is minimized using user-identified criteria, and any pixels beyond a set similarity threshold are merged into adjacent image segments. Each segment contains statistical attributes, including the internal pixels’

histogram and additional information derived from the image object such as texture, segment size and shape, and relationships to object super or sub-classes (Fournier et al, 2007; Hess et al, 2003; Repaka et al, 2004). Second, object-oriented classifications take advantage of the variety of available segment statistics in order to split the segments into information classes. Wetland segmentation could also integrate GIS and other ancillary data sources to identify the spatial extent of wetlands (Fournier et al, 2007; Huan and Zhang, 2008). Hess et al (2003) and Grenier et al (2007) both found segmentation to be highly accurate for partitioning wetland and non wetland areas (95% and 80% accuracy, respectively). This effort focuses only on image segmentation to facilitate wetland mapping and not automated object classification.

### 2.2.2. Segmentation Methodology

The segmentation parameter settings best attuned to wetland delineation depend greatly on the spatial and spectral resolution of the images to be segmented and the size of the features to be identified. Optimal settings would yield an image segmentation with polygons small enough to capture the smallest target features, yet large enough to prevent shadows from being isolated into individual polygons. Under the FGDC Wetland Mapping Standards, the primary imagery for wetland delineation and classification must have a spatial resolution of at least one meter or smaller, is recommended to include a color infrared band, and must identify 98% of wetlands larger than 0.5 acres or 2023.4 square meters (FGDC, 2008). To meet these requirements, all segmentation parameter trials were conducted with a subset of the USDA Farm Service Agency's one meter resolution color-infrared National Agricultural Imagery Program (NAIP) imagery.

We used a multi-resolution image segmentation algorithm (Definiens Professional Version 5) to test image segmentation for wetland mapping. Within the segmentation algorithm, four adjustable parameters can be used to adjust the size of the segmented polygons and determine how the segments are calculated (Figure 13). The scale parameter sets a limit on the heterogeneity within each segment. The higher the scale parameter is set, the more within-segment variation is allowed, and the larger the relative range of polygon sizes. Low scale parameter values (10-20) result in small image objects relative to the image pixel size, while large scale parameter values (100) result in very large super-objects than can be further broken down by successive segmentations. Though adjusting this parameter provides a fast way to create larger image objects, its purpose is to ensure that the pixels within each object are truly related; object size can be increased by merging adjacent segments together when necessary (Definiens AG, 2006).

The other three parameters determine the ratio of color or shape used to segment polygons and the degree of polygon compactness and smoothness imposed upon the polygons (Figure 13). A color and shape criterion identifies the relative importance of shape and spectral information used to create homogeneous segments. The total parameter must always equal 1, so when shape is maximized (0.9), color comprises only 0.1 of the calculation and when color is maximized (1), only color is used to calculate segment homogeneity. A balanced segmentation would utilize both shape and color at 0.5 to create segments. When the shape parameter is higher than zero, compactness and smoothness are invoked to set limits on long or narrow features as well as features with very rough boundaries, respectively (Definiens AG, 2006).

In addition, ancillary vector and raster data including GIS layers, actively sensed radar and LIDAR data, and additional remote sensing imagery at varied spatial resolutions can be integrated with the primary imagery during segmentation without resampling or degrading the ancillary data quality (Fournier et al,

2007; Huan and Zhang, 2008). It should be noted that while data with any spatial resolution can be input to a segmentation algorithm, pilot tests suggest that the spatial resolution of included ancillary data should be similar in resolution to the primary segmentation imagery. Tests using 24 meter CTI data resulted in very angular, polygonal boundaries between segments rather than the natural, smooth boundaries desired for wetland delineation (Figure 14). In Definiens Professional 5, ancillary data layers and primary imagery bands can also be weighted to allow certain layers a greater influence on the resulting segmentation. For example, RADAR and NDVI layers may provide key information for identifying forested wetlands, and could be weighted twice as high as accompanying infrared or green bands.

In the case of wetlands, image segment need enough internal variation to encompass spatially heterogeneous wetlands. For example, many wetland classes include patches of open water and vegetation that would be misclassified by a per-pixel classifier. The scale of the image segments should be large enough to include such patchiness within a single segment, which may also require creating multiple image segmentations with different scale and homogeneity parameters to accommodate wetland types with various amounts of internal patchiness or spatial heterogeneity (Fournier et al, 2007; Huan and Zhang, 2008; Grenier et al , 2007). In per-pixel classifiers, a vegetation patch can be identified reliably only when pixels fall within ½ to ¼ of the patch’s size (Hunt et al, 2007). If the same logic also holds for identifying patches using image segments, then the 0.5 acre (2024 square meter) target wetland mapping unit can be identified by image segments covering at least 500-1000 square meters.

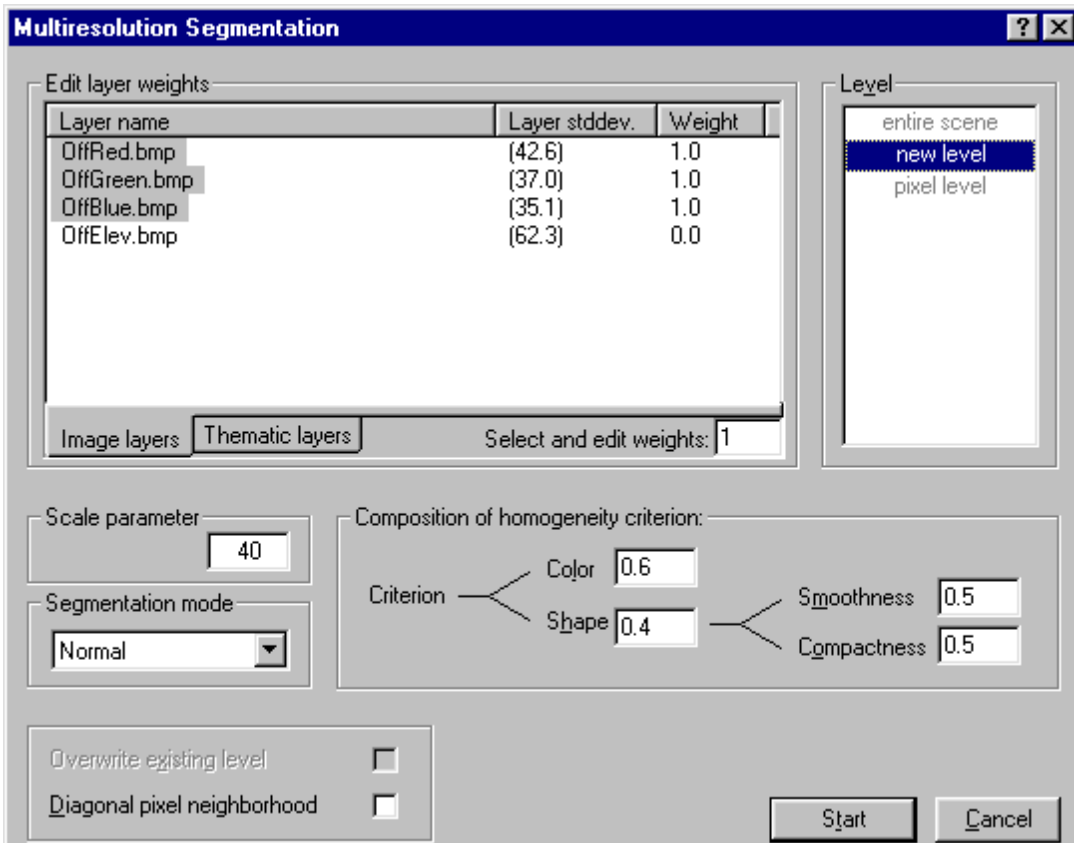
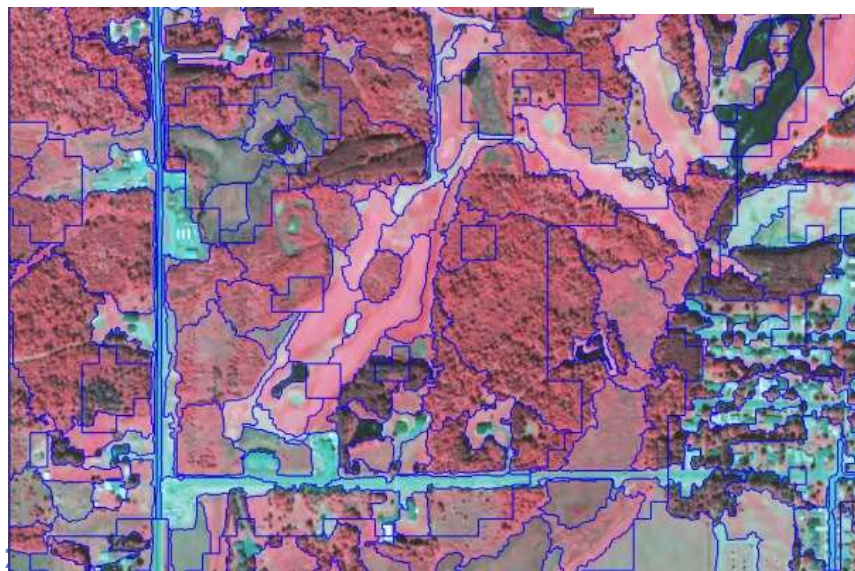


Figure 13. Multi-resolution segmentation dialog box from Definiens Professional 5. (From eCognition (aka, Definiens) basic training, URL [http://www.rstc.msstate.edu/wfd/ecog/docs/course\\_material.pdf](http://www.rstc.msstate.edu/wfd/ecog/docs/course_material.pdf))



Figure 14. Images showing (*top*) the 24 meter CTI, with green areas corresponding to potential wetlands; (*middle*) the result of a segmentation including the CTI data, with each segment outlined in black; and (*bottom*) the segments shown with the image they were derived from. As you can see, the CTI blocks are very large and oddly shaped compared to the rest of the segments and do not accurately conform to the wetland's natural boundaries.



A series of segmentation trials were completed with a subset of the 2008 CIR NAIP imagery for Cloquet, Minnesota. Selected results showing the effects of the scale parameter value and the shape/color parameter on resulting image segmentations can be seen in Table 5 and Figure 15. As expected, the lowest scale parameter (10) created the largest number of image segments. This scale parameter was a poor choice for wetlands: the segments were more than five times smaller than the minimum wetland size and unnecessarily separated shadows as unique features. At the highest scale parameters (75-100), the opposite was true and segments included so much internal variation that visually distinct classes were aggregated. The optimal scale parameter (50) identified 2-4 times the number of segments as the 100 scale parameter, and 23 times less than the 10 scale parameters. It should be noted that due to a

random seed used during segmentation, even when repeated with the same imagery and the same parameters, will produce slightly different segment boundaries and a slightly different number of image objects. The differences get more pronounced as segment size (scale parameter value) decreases, so that at a scale of 100, the segment boundaries are nearly identical and at a scale of 50, only 36% of image objects remain identical.

Shape and color parameter combinations tested with the 50 scale parameter value are also shown in Table 5 and Figure 15. The most highly shape-dependent segmentation scheme (shape .9, color .1) was almost entirely calculated based on shape, resulting in very compact polygons with few long or narrow areas identified only when extremely spectrally unique (such as the roads in Figure 15). Segmentation based primarily upon color (shape .1, color .9) creates polygons with a wider range of sizes and splits polygons that otherwise appear spectrally similar. The balanced approach with shape and color at .5 emphasizes internal spectral homogeneity while allowing the shape parameter sufficient flexibility to group wetland patches with slightly different spectral signatures. The 50 and 75 scale parameter segmentations fit the minimum wetland area (patch identification) requirements very well, and the balanced color and shape parameters ensure segment polygons based solidly upon internal spectral homogeneity while creating polygons of similar sizes.

**Table 5. Parameters for multi-resolution segmentation trials in Definiens Professional 5. The area column refers to the range of areas in pixel objects containing field GPS points (presumably, wetland objects). Total image area of the NAIP image subset is 27,751,825 square meters.**

Scale Parameter	Shape /Color	Compactness and Smoothness	No. of segments in subset	Area (m <sup>2</sup> )	Comments
10	.5/.5	.5	544,324	61-107	Objects much too small. Shadows become independent features rather than blending in. Very low segmentation heterogeneity threshold results in many very similar and adjacent polygons.
50	.5/.5	.5	23,667	796-8135	Can still pull out very small homogeneous areas (35 pixels for a pond, for example). Shadows are no longer unique features. Segmentation no longer artificially splits similar areas. Highest detail of the three 50 scale tests.
50	.9/.1	.5	13,419	796-10593	Higher focus on the shape homogeneity in resulting objects, which tends to merge otherwise spectrally unique polygons.
50	.1/.9	.5	10,156	796-14386	Higher focus on spectral homogeneity, which merges areas of like color and splits those slightly different.
75	.5/.5	.5	13,170	1483-13640	Larger objects with high internal heterogeneity.
100	.5/.5	.5	4936	1485-23123	Much larger objects with very high internal heterogeneity. Many image objects were lumped with fairly spectrally different, though adjacent polygons.

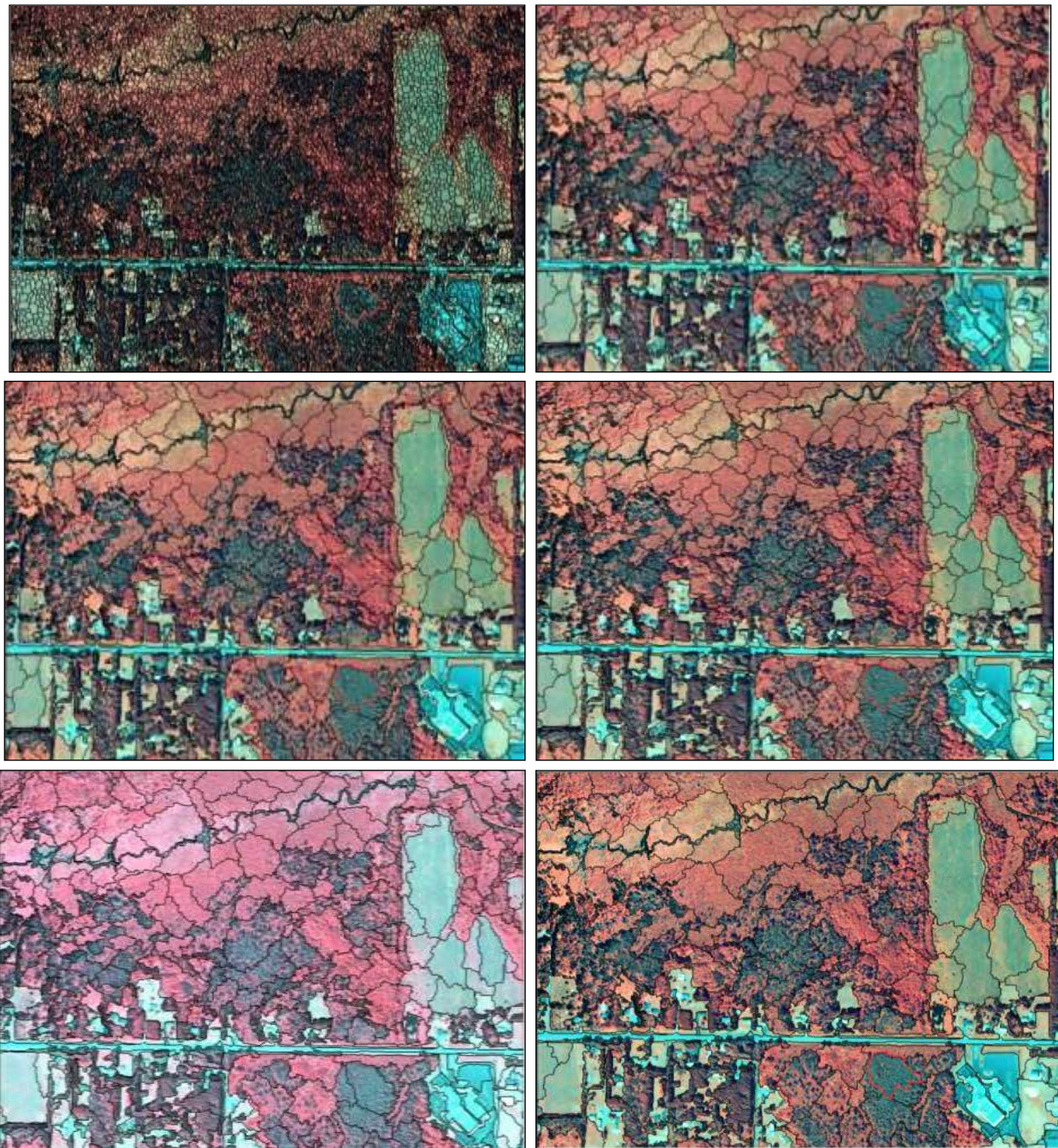


Figure 15. These images show the affects of various segmentation parameters on the size and location of segment boundaries in the one meter 2008 CIR NAIP imagery. From top left, (*top row*) scale parameter 10, balanced shape and color (.5 each) and scale 50, balanced shape and color, (*middle row*), scale 50, shape .9, color .1 and scale 50, shape .1 color .9, (*bottom row*) scale 75, balanced shape and color and scale 100, balanced shape and color.

In-depth visual assessments of the various segmentation results identified the segmentation with scale parameter 50 and balanced color and shape parameters as the best fit with one-meter CIR NAIP imagery. In this segmentation, the locations of polygon boundaries and segment sizes adequately fit the photo-interpreted land use and land cover. The segments successfully delineated roads, fields, forest stands, wetlands, water bodies, and urban areas, and also separated natural land cover categories, such

as open water and floodplain meadow or deciduous and evergreen forests. To further examine the segmentation boundaries for wetlands, the image objects were compared against the current National Wetland Inventory (NWI) vector data for Cloquet, MN. To directly compare the segmentation against NWI data, the segmented layer was first exported to a vector layer and input into ArcGIS. The NWI layer was then used as a template to select wetland segments touching the NWI polygons. As is shown in the series of figures below, the wetland polygons from the segmentation layer include water bodies and split wetland vegetation from upland vegetation extremely well (Figure 16). In many areas, the segmented wetland polygons identified obvious wetlands that the NWI omitted and delineated the wetland boundaries with more realistic, natural variations and much higher detail than the NWI.

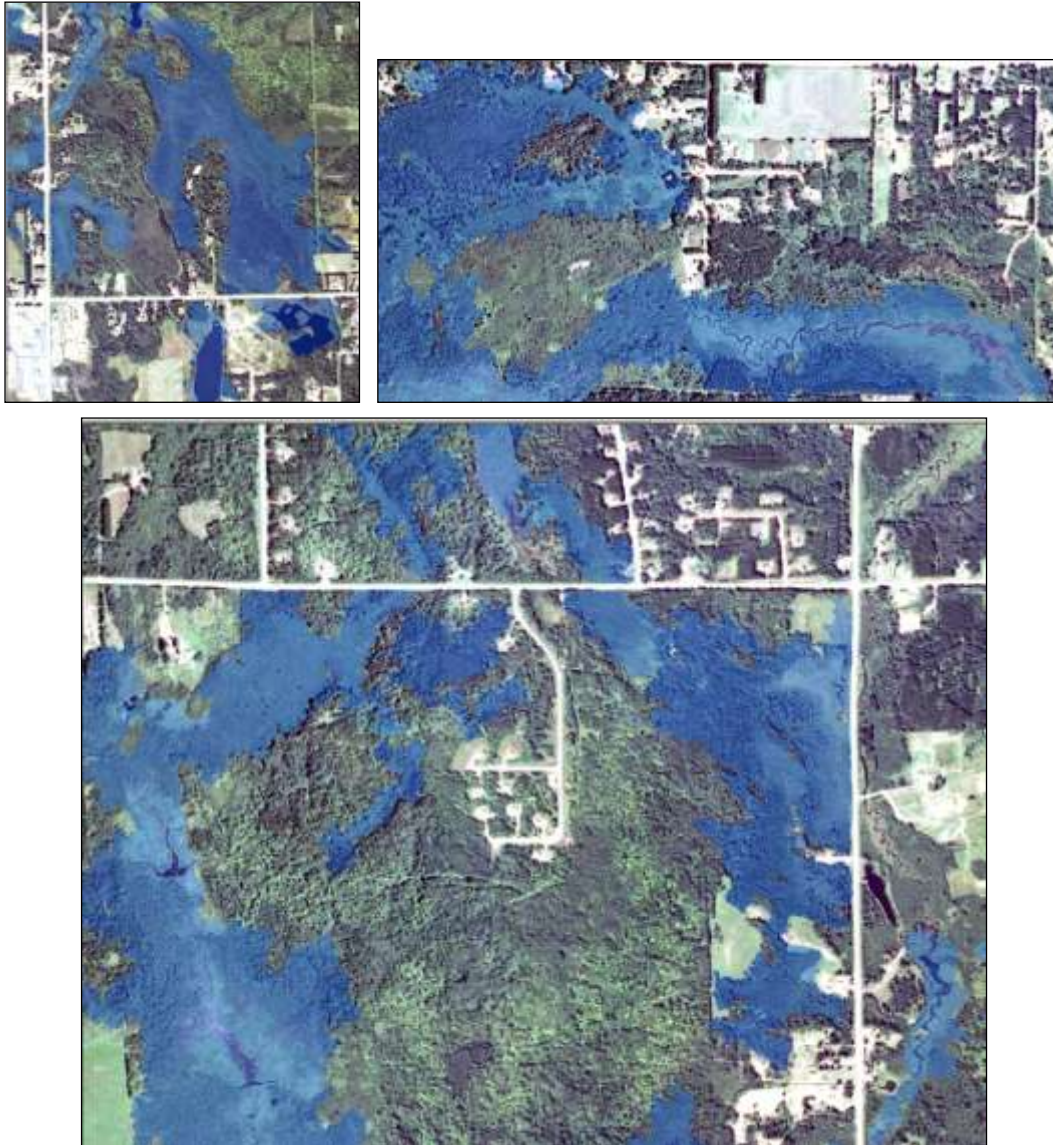


Figure 16. The blue areas correspond to Definien's Professional 5 wetland polygons. Included polygons overlapped with areas within the NWI layer.

#### 2.2.4. Segmentation Discussion

Depending on the scale parameter setting and the size of the image, segmentation can be extremely time consuming and computationally expensive. Attempts to segment the entire county composite image were unsuccessful due to limitations in computing power; however, processing of USGS quarter quad tile images were feasible with a desktop computer. Despite the additional time required to segment the imagery, working with image objects rather than individual pixels for wetland classification would significantly reduce the overall time necessary for wetland mapping and classification (Meinel and Neubert, 2004).

The benefits to be gained from segmentation are well worth the added processing steps. Segments can be easily converted to vectors and brought into alternate software programs. Definiens exports vector polygons in shapefile format, which would make them usable in ArcGIS, ERDAS Imagine, and most other GIS packages (the shapefile vector data format is an Open Geospatial Consortium standard format, which means the source code is universal and public, and ensures that the majority of GIS packages can read them).

When working from the segment layer, wetland delineators have only to select, copy, and paste a segment or set of segments to add them to the NWI polygon dataset. The hybrid process of segmentation and manually editing, merging, or clipping wetland polygons would be much faster, since the segments provide delineators with a ready starting point (Hess et al, 2003). As noted above, the segmented polygons include much more spatial detail and finer-scale edge delineation than polygons currently in the NWI dataset. This extra detail may increase the overall accuracy of the NWI at local scales by accounting for seasonal variations and small but important drainage systems otherwise omitted by the NWI. Because the wetland delineation process is automated, Definiens Professional 5 could be used to both increase wetland boundary detail in the NWI and to keep that level of detail consistent among different interpreters. Even if the level of detail is too high for the NWI, any segmented polygons added to the NWI could be simplified and smoothed in ArcGIS – a process which could easily be automated – prior to manual editing. Overall, using Definiens software to obtain wetland boundaries either should reduce or eliminate the need for manual edge editing of wetland polygons in the NWI.

Since the segmentation uses the spectral data to segment the landscape, any wetlands (regardless of location or surrounding land use) with unique spectral characteristics should be discernable with the right combination of imagery and ancillary data. However, to delineate wetlands beneath a forest canopy, leaf-off imagery or radar capable of penetrating the canopy would be a prerequisite to accurate segmentation. As long as a wetland is large enough to be detected at the imagery's spatial resolution, ancillary remote sensing and other data should be sufficient to delineate the wetland, though classification requires a much more specific set of spectral bands and ancillary data to classify wetlands with any degree of accuracy. When combining images, mosaicking and histogram matching may be necessary to ensure that the segments do not identify image edges as segment boundaries.

Care should be taken to ensure that the tiles are edge matched. Edge matching algorithms available.

## 2.3. Wetland Typing using Decision Trees

### 2.3.1. Wetland Typing Introduction

The mapping of wetlands boundaries is only one goal of the National Wetlands Inventory (NWI). Additional wetland characteristics such as classification type are also important goals. The current NWI characterizes wetlands using the Cowardin classification system (Cowardin et al., 1979) and the U.S. Fish and Wildlife Service (USFWS) Circular 39 classification system (Shaw and Fredine, 1971); however, Minnesota's wetland regulatory agencies have begun advocating the use of wetland plant community types (Eggers and Reed, 1997) for use in wetland delineation and permitting. Further work will be required to include it in a future update of the NWI.

There are many remote sensing classification techniques, each with unique advantages and disadvantages. An unsupervised classification is one common technique (Ozesmi and Bauer, 2002; Sader et al., 1995). Unsupervised classification is often applied because it eliminates the need for a time consuming training step. Hybrid classifications, described by Jensen (2005), combine unsupervised clusters with supervised training sets of known land cover. The training phase involves defining spectral signatures of known land cover and then incorporating those signatures into a classification model, typically done using the ERDAS software package. Other classification methods use image derivatives to discriminate image texture. Vegetation indices such as the normalized difference vegetation index (NDVI), the TM Band 4:5 ratio, and the TM tasseled-cap model are used as textural information to further discriminate wetlands, particularly forested wetlands (Wright and Gallant, 2007; Hodgson et al., 1987). Automated processes, however, tend to confuse some types wetlands with other land cover classes. This is particular problem with wetland classification because of the temporal variability of wetland characteristics over the course of a growing season and is especially a problem with forested wetlands whose tree canopies have spectral reflectance characteristics similar to upland forests.

In addition to automated processes, visual interpretation of imagery can be a useful element in the classification process. Harvey and Hill (2001) reported that these semi-automated maps resulted in wetland maps that were 9% more accurate results than completely automated approaches. An expert classifier is one that is guided by an interpreter, the "expert," and can incorporate attributes such as image texture, topography, and other GIS based datasets that can aid the automated processes with the hope of ultimately increasing classification accuracy. The Knowledge Engineer, an ERDAS software product, is an expert classifier that was evaluated in this study. An expert classification system was chosen because of its ability to combine traditional automated processes with expert knowledge to provide the optimal accuracy and efficiency in classifying wetland type. This study will focus on classifying seven Eggers and Reed forested wetland types: deciduous forest, floodplain forest, shrub carr, alder swamp, coniferous swamp, coniferous bog, and open bog.

### 2.3.2. Wetland Typing Methods

#### 2.3.2.1. Field Data Collection

The Fond du Lac Reservation, located northwest of the City of Cloquet, Minnesota, was selected as the pilot study area because of the availability of high quality GIS data sets, namely a reservation wide wetland inventory completed in 2008 and high resolution (2 ft) topography data. A field study was conducted July 13-17, 2009 by researchers from the University of Minnesota, including one MN Certified

Wetland Delineator. 250 points were randomly generated within wetland types in a stratified random sampling scheme. The points were loaded into Trimble GeoXT and GeoXH handheld GPS units, which are sub-meter accurate under optimal conditions. A minimum of 50 positions were collected for each GPS point collected during the field study. Data were post processed and corrected using Pathfinder Office.

### *2.3.2.2. Imagery and GIS Data Layers*

Two primary sources of aerial photography were used throughout the study. The National Agriculture Imagery Program (NAIP) imagery from 2008 has four spectral bands (B, G, R, NIR), a spatial resolution of 1m, and was collected mid to late August in the study area. In addition, the MN Department of Natural Resources (DNR) acquired imagery flown by Keystone Aerial Surveys Inc. in May 2009, prior to leaf out in the study area. This imagery has four spectral bands (B, G, R, NIR) and a spatial resolution of 0.5m.

Other data sets that currently comprise variables in the decision tree include the Natural Resources Conservation Service (NRCS) Soil Survey Geographic (SSURGO) Database, specifically spatial data and soil pH attributes, and the compound topographic index (CTI) that can be used as a measure of soil wetness. In addition, a wetland inventory was completed in 2008 in the area of the Fond du Lac Reservation. This dataset was used in preliminary decision tree development.

### *2.3.2.3. Conceptual Decision Tree*

A conceptual tree was constructed in order to visualize the classification process. Figure 17 is the conceptual tree for forested wetland classification, based on Eggers and Reed's (1997) wetland community classification key. The tree does not follow the Eggers and Reed key exactly, as each directional node in the tree must be based on a difference in vegetative cover detectable by remote sensing or another GIS variable.

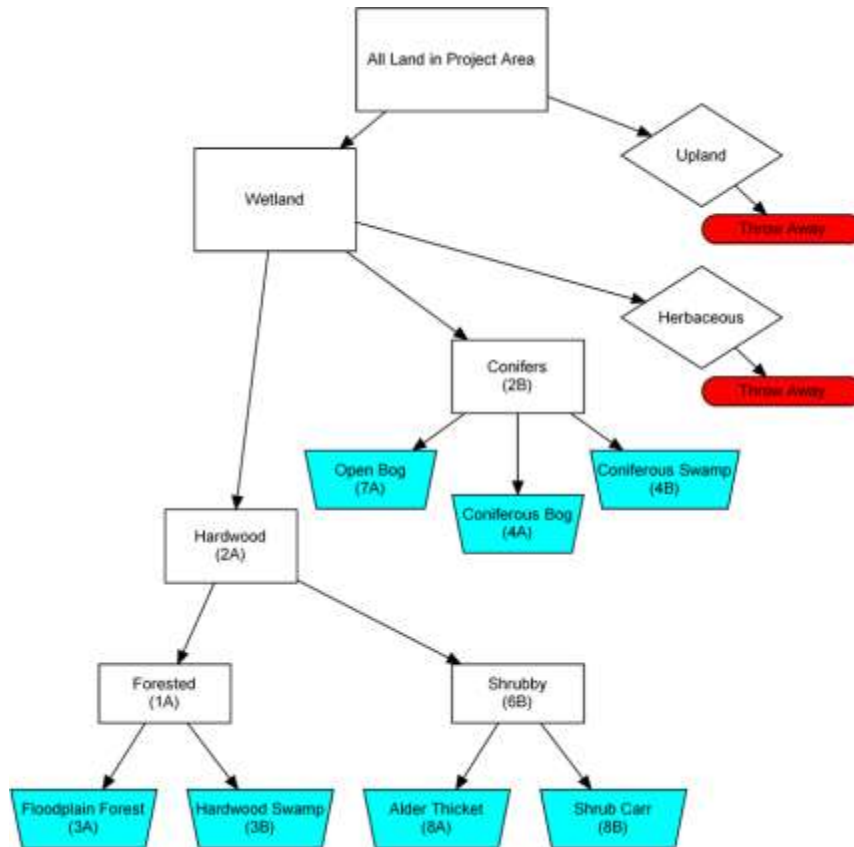


Figure 17. Conceptual classification tree for Eggers and Reed wetland types.

#### 2.3.2.4. Determination of Variables

A portion of the field collected data was used in combination with imagery and ancillary GIS data sets to examine potential differences between wetland types. Eighty-one polygons were created around wetland points of different classes. Polygons were created manually by an interpreter to ensure wetland homogeneity. These polygons were used to generate statistics for a number of variables in an effort to distinguish between wetland types. Polygons were also created using Definiens eCognition software and then those polygons surrounding the wetland points were extracted and aggregated by wetland type. Statistics based on interpreter and eCognition polygons were examined. The high resolution imagery was degraded to 1m and 3m data sets in order to decrease the effects of solar angle, shadows, and speckle common to imagery with very high spatial resolution.

Statistics have been generated for the following attributes for use in the decision tree classifier:

- individual B, G, R, NIR bands for 2008 NAIP imagery and 2009 leaf off imagery
- NDVI for 2008 NAIP imagery and 2009 leaf off imagery
- NDVI difference image (leaf on – leaf off)
- Soil pH

#### 2.3.2.5. ERDAS Knowledge Engineer

ERDAS Knowledge Engineer is a per pixel decision tree based classifier that is comprised of end or intermediate hypotheses, rules, and variables. End hypotheses are output classes from Knowledge Engineer, in this case the end hypotheses are the seven Eggers and Reed forested wetland types. Intermediate hypothesis are classes that are nodes in the decision tree but not output from the model, such as coniferous and deciduous land cover, from which further classification can take place. Hypotheses are evaluated by rules, which determine whether or not an input variable meets a given criterion. A variable can be defined from a raster or vector data set. For example, a variable could be the calculated NDVI layer, and a rule could be that if the NDVI value for a pixel is greater than 0.4 then it would fall within the intermediate hypothesis of vegetation. The decision tree is based on a logical progression. All variables must be verified if a rule is to be correct, and a hypothesis is true if one or more rules relating to the hypothesis are correct. Figure 18 shows the decision tree being developed for this study.

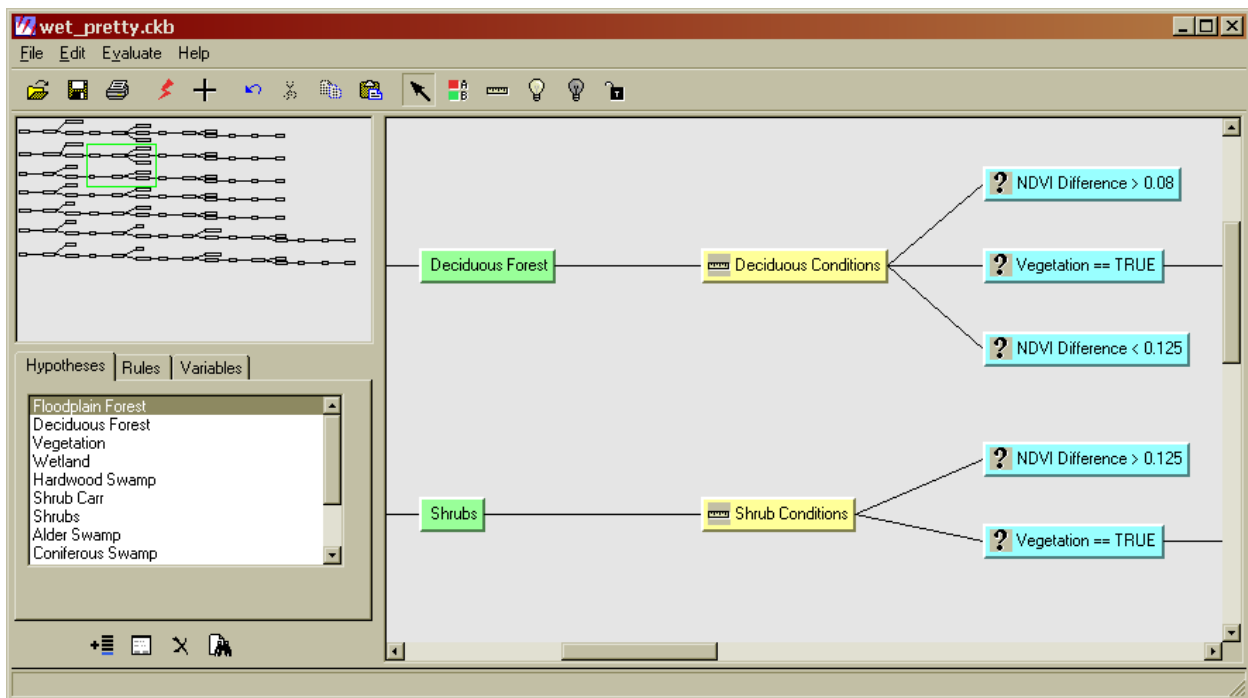


Figure 18. Sample variables, rules, and intermediate hypotheses in ERDAS Knowledge Engineer.

### 2.3.2.6. Accuracy Assessment

Accuracy assessments were conducted using 146 field collected, forested wetland points. A 10m buffer was created surrounding each point, and accuracy was assessed based on the majority of the classified wetland type within the buffer. This method ensures classification homogeneity, reduces errors due to GPS inaccuracy, and reduces the chance that a single pixel classified incorrectly in a group of correctly classified pixels negatively affects the accuracy assessment.

### 2.3.3. Wetland Typing Results

### 2.3.3.1. Data Collection

GPS post processing accuracy reports show that approximately 50% of positions collected were sub-meter accurate, approximately 80% of positions were accurate to two meters, and approximately 96% of positions were accurate to five meters. Table 6, below, is an example of the field data collected. A total of 151 wetland (146 forested) and 31 upland data points were collected.

Table 6. Sample of wetland data collected during July, 2009.

ID	Wet/Up	Eggers & Reed Type	Cowardin Type	Cowardin Hydrology	Vegetation
11	Wetland	Open Bog	PEM3	B	labrador tea, bog rosemary, sphagnum
14	Wetland	Shrub-Carr	PSS1	B	dogwoods, other mixed deciduous shrubs
260	Wetland	Alder Thicket	PSS1	B	alder, some spruce, tamarack
15	Wetland	Alder Thicket	PSS1	B	alders, some dogwood, sedge, bluejoint grass
362	Wetland	Hardwood Swamp	PFO1	B	black ash, birch, maple, some alder
101	Upland				red pine plantation, no understory vegetation
67	Wetland	Coniferous Bog	PFO2	B	tamarack, bog rosemary, labrador tea, black spruce
64	Wetland	Coniferous Bog	PFO2	B	tamarack, bog birch, alders
97	Upland				area of aspen regrowth, scattered red pine and basswood
60	Wetland	Coniferous Swamp	PFO4	B	cedar, balsam fir, tamarack, sedge
112	Wetland	Coniferous Bog	PFO2	B	tamarack, black spruce

### 2.3.3.2. Determination of Variables

Image statistics for interpreter and eCognition polygons were examined. eCognition polygons exhibited a different mean, higher variability, and higher standard deviation than those created manually by the interpreter. Further statistics used in determining differences between vegetative classes were calculated using the interpreter based polygons.

Image statistics for 1m and 3m degraded images were examined. Statistics calculated for data sets degraded to 3m showed less variability and smaller standard deviations per wetland class, and thus the high resolution images were degraded to 3m for further classification. Degradation reduces noise in the data and decreases the computer processing time considerably.

Image statistics for several variables were examined. Differences were found between vegetative classes, and the following describes the use of variables in the decision tree classifier:

- The NIR band was extracted from both the 2008 NAIP leaf on image and the 2009 leaf off image. The lowest NIR value was 23 for all wetland classes. All NIR values less than 23 were assumed to

be water, as clear deep water reflects NIR very poorly, and were not included in the decision tree.

- The NDVI was calculated for the 2008 NAIP leaf on imagery and normalized to a 0 – 1 scale. This gives a good indication of maximum annual greenness, as the imagery was flown during late summer. If an NDVI value was low for the leaf on image, it can be generally assumed that the area is not vegetated at any point during the year.
- The NDVI was calculated for the 2009 leaf off imagery and normalized to a 0 – 1 scale. This gives a good indication of minimum annual greenness, as the imagery was flown prior to deciduous leaf out. A high NDVI value for this date is generally indicative of evergreen vegetation.
- An NDVI difference image was created by subtracting the leaf off NDVI from the leaf on NDVI. This eliminates background greenness that is present year round. A high NDVI difference value indicates substantial vegetative growth. Figure 19 shows the NDVI difference for six wetland classes (hardwood swamp and floodplain forest are lumped into a deciduous forest category). The mean NDVI difference values for the deciduous and coniferous classes were 0.15 and 0.01, respectively. The NDVI difference value is used to distinguish deciduous and evergreen classes in the decision tree.

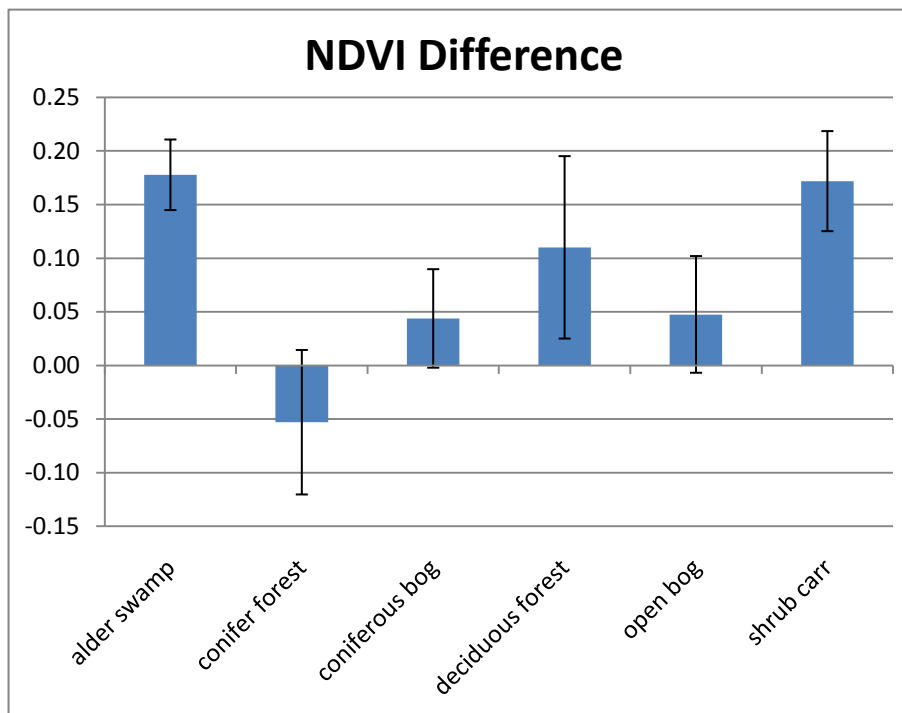


Figure 19. NDVI difference for six wetland classes. Error bars are one standard deviation.

- Soil pH for each class was derived from the SSURGO database and was used to distinguish coniferous and open bogs from coniferous swamps. The mean soil pH for the coniferous swamps was 4.36, while the mean soil pH for the coniferous and open bogs combined was 3.86. It is noted that shrub carr and alder swamps also tend to have a low pH but have already been separated as deciduous vegetation at this point.
- Subtle differences were noted in some of the individual bands that could be used to differentiate wetland classes, specifically coniferous and open bogs as well as alder swamps and shrub carrs. The mean leaf off NIR value for shrub carrs and alder swamps were 162 and 182,

respectively. The mean leaf off B band value for coniferous bogs and open bogs were 119 and 138, respectively. However, these differences alone are weak and additional discriminatory variables will be needed for adequate class separation.

### 2.3.3.3. ERDAS Knowledge Engineer

The ERDAS Knowledge Engineer uses a linear model of the variables, rules, and hypotheses for each class rather than a bi-directional decision tree (Figure 18). This makes it difficult to visually assess the model as a whole. A binary decision tree better represents the process (Figure 20).

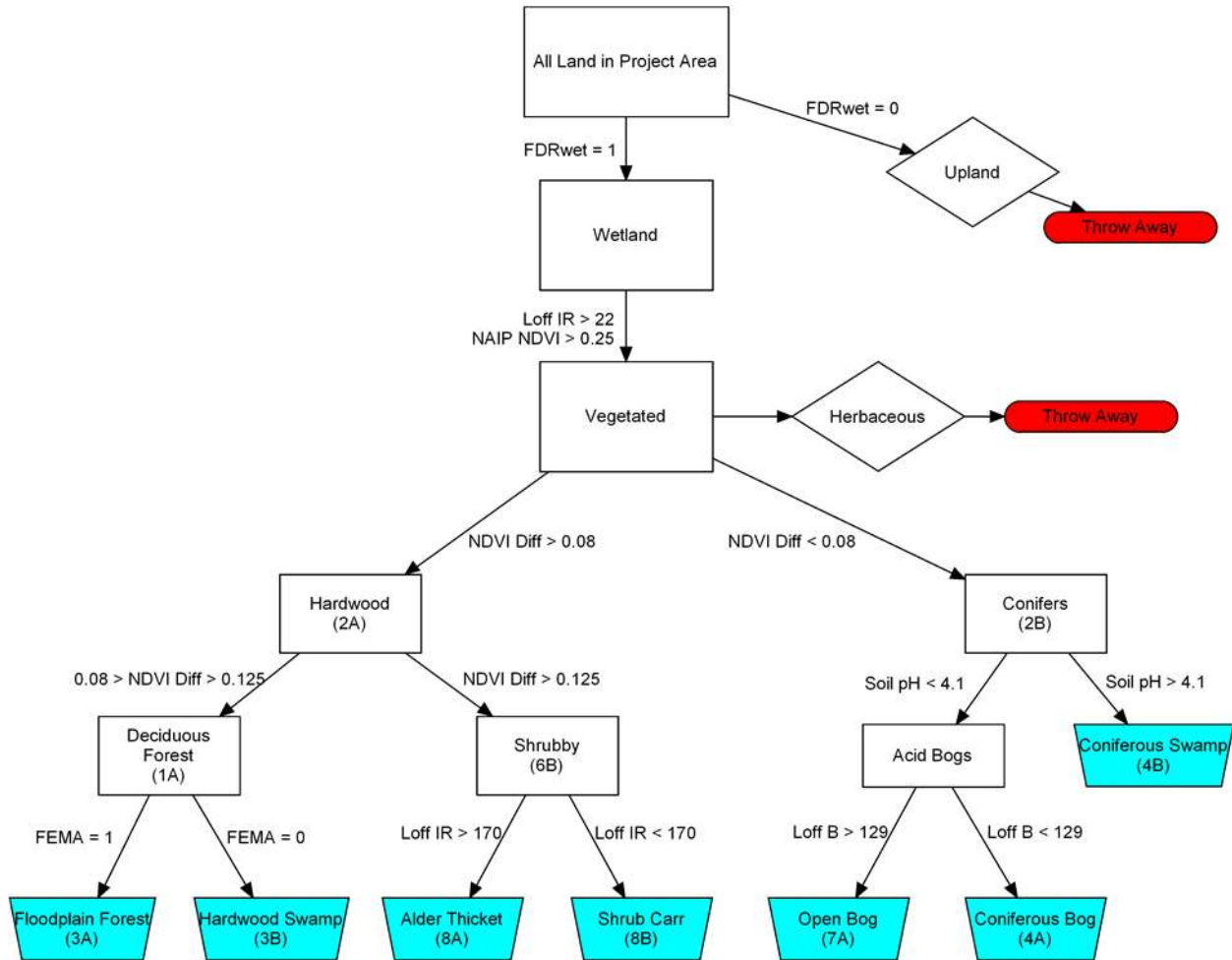


Figure 20. Draft decision tree used for wetland classification.

### 2.3.3.4. Classification

The results of the preliminary classification are shown in Figure 21, below. Figure 22 is a zoomed portion of the classification map.

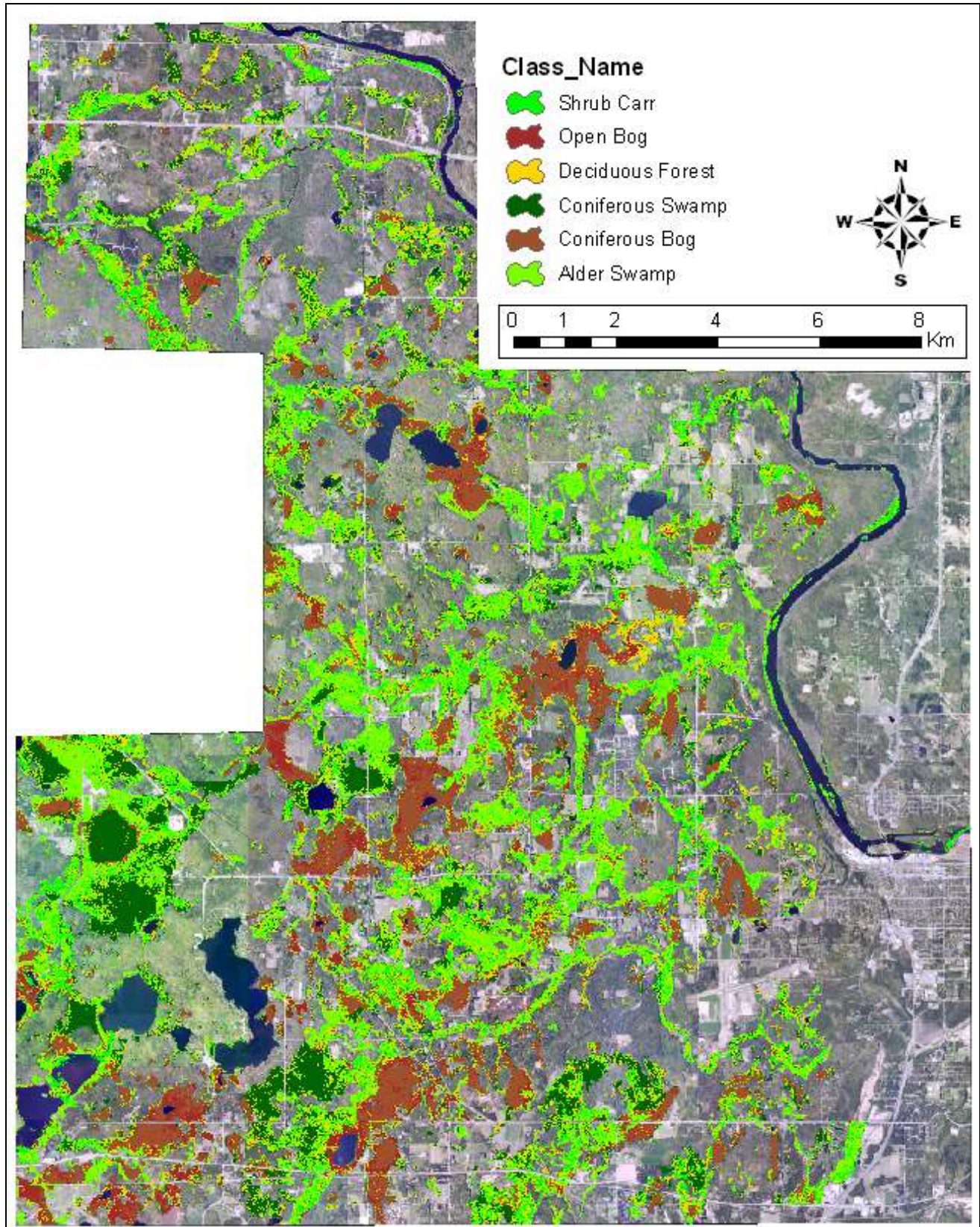


Figure 21. Preliminary forested wetland classification map.

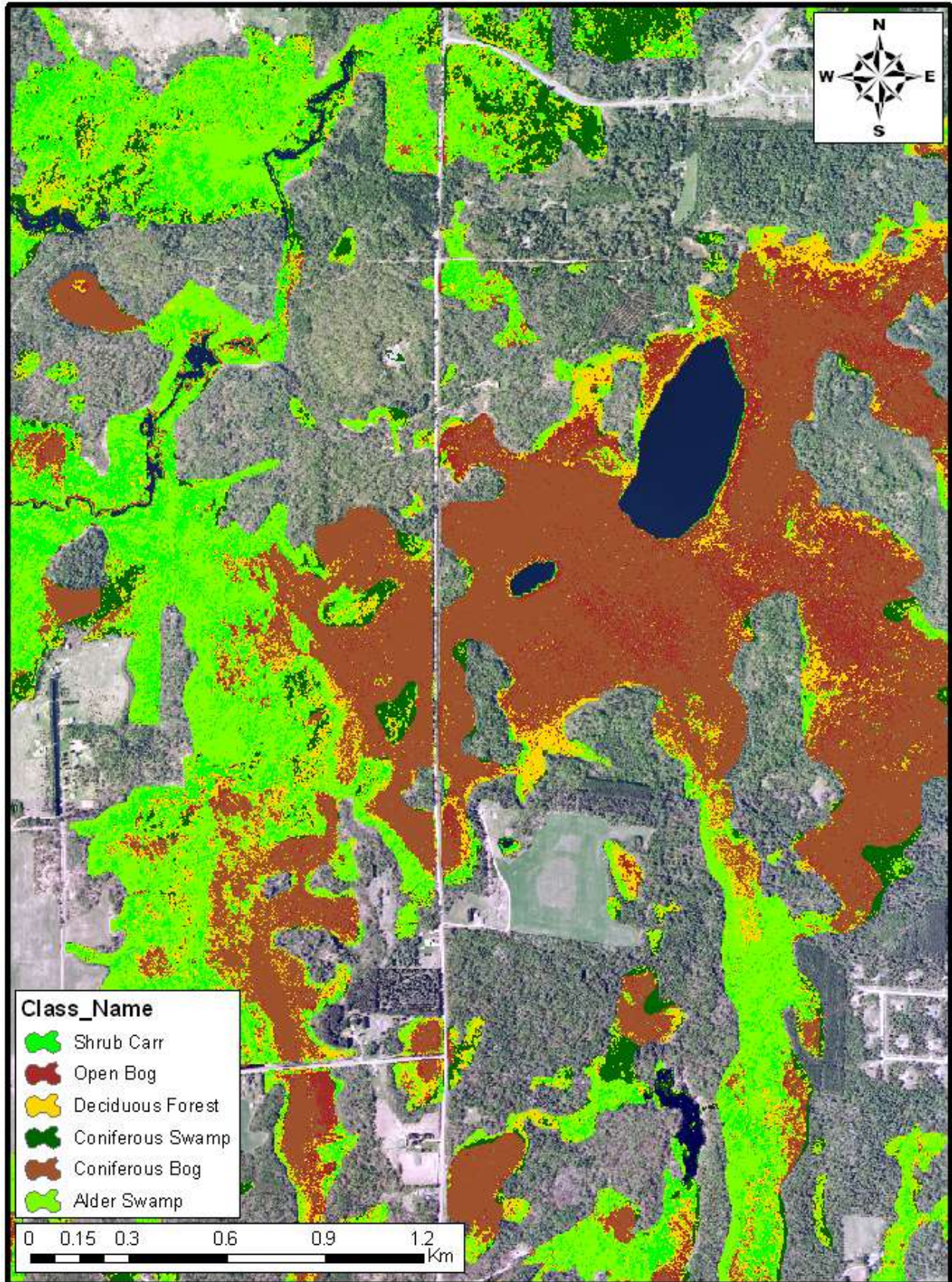


Figure 22. Zoomed portion of preliminary wetland classification map.

### 2.3.3.5. Accuracy Assessment

The overall accuracy of the preliminary decision tree classifier was 47.9% (Table 7).

Table 7. Error Matrix for preliminary forested wetland classification.

		Reference Data							Total	User's Accuracy
		HW Swamp	Shrub Carr	Alder Thicket	Conif. Swamp	Conif. Bog	Open Bog			
Map Data	HW Swamp	11	4	4	4	2	1	26	42.3%	
	Shrub Carr	15	9	4	0	0	0	28	32.1%	
	Alder Thicket	8	20	13	0	0	1	42	31.0%	
	Conif. Swamp	1	0	0	9	5	0	15	60.0%	
	Conif. Bog	0	0	0	3	23	0	26	88.5%	
	Open Bog	0	0	0	0	1	2	3	66.7%	
	Totals	35	33	21	16	31	4	141		
	Producer's Accuracy	31.4%	27.3%	61.9%	56.3%	74.2%	50.0%			
Overall Accuracy									<b>47.9%</b>	

### 2.3.4. Wetland Typing Discussion

#### 2.3.4.1. Data Collection

At the time of the field study, the open bog class was not considered for classification. Future iterations of the forested classification decision tree may not include open bogs because of the lack of reference information. Reference information may also be obtained using the Minnesota County Biological Survey (MCBS) dataset.

#### 2.3.4.2. Determination of Variables

The determination of variables is the major shortcoming of the wetland classification process thus far. There are multiple steps that require improvement, perhaps most importantly the removal of emergent vegetation from the “vegetation” intermediate hypothesis. The model currently overestimates shrub carr and alder thicket, and qualitative investigation shows that many of these areas are actually wet meadow, shallow marsh, or other vegetative communities dominated by herbaceous cover. Analysis of imagery statistics for herbaceous wetland classes will be examined and a rule for removal of herbaceous vegetation will be established in future iterations of the decision tree model.

Currently the model relies on the Fond du Lac wetland inventory to determine if an area is wetland or upland. The inventory was created by expert interpreters and thus the confidence of the wetland/upland discrimination power of the inventory is high. The inventory has been helpful in model development for this specific area, but no such data set exists throughout Minnesota. The use of the CTI

to discriminate wetland and upland is being evaluated and will be incorporated into future iterations of the decision tree model.

The current version of the model does not discriminate floodplain forests and hardwood swamps. Analysis of imagery statistics reveals that these two wetland classes have very similar spectral reflectance characteristics and it is not possible to confidently distinguish between these floodplain forests and hardwood swamps using imagery alone. Ancillary data sets based on topographic data are being evaluated.

The current version of the model relies on several weak differences between classes, including those based on single band imagery and on soil pH. Soil pH data are taken from the SSURGO dataset, which maps soils at a landscape scale. Fine scale pH differences will not be distinguishable using this data set. Furthermore, soils data are not yet available statewide in digital formats, although the development of digital data is ongoing. Further investigation will be conducted to determine differences between wetland types that can be combined with soils and single band image data to provide a more confident distinction of wetland classes.

The use of radar data is also being evaluated for its use in discriminating vegetated wetland classes. Numerous studies (Hess et al., 1990; Hess et al., 1995; Whitcomb et al., 2007; Henderson and Lewis, 2008) report the usefulness of radar data in discriminating between wetland and upland, as well as vegetative species differentiation. Future studies will be conducted to determine the usefulness of radar data in the Fond du Lac study area. However, radar images are not currently available statewide and are expensive to obtain.

The expert classification and decision tree methods allow for a variety of local data to be used when discriminating wetland types. The applicability of data varies throughout the state depending on dominant land use. Remote sensing techniques that distinguish forested wetland types may need to be further refined in the northern lakes and forests region, whereas springtime determination of agricultural wetlands will likely be the focus of the studies in the western corn belt plains. The expert classifier model allows for use of data sets that are the most applicable for a particular area.

### **2.3.5. Wetland Typing Conclusions**

As shown in Table 7, the overall accuracy of the preliminary forested wetland classification is 47.9%, which is not adequate to meet the FGDC mandated thematic accuracy standard of 85%. Further modeling is expected to enhance the accuracy somewhat. Accurately classifying forested wetlands is a difficult task for a variety of reasons, and further investigation will be needed to determine whether it is possible to confidently and accurately classify forested wetlands without expert interpretation using Knowledge Engineer or other expert classifiers. The availability of high resolution leaf off and leaf on aerial photography as well as high resolution topography data has the potential to be the basis for more accurate automated classification. Further investigation will continue with the goal of determining this potential.

## **2.4. Wetland Mapping using RADAR Imagery**

### **2.4.1 Introduction to Wetland Mapping with Radar Imagery**

Wetland boundaries are dynamic in both space and time, with fluctuation depending on many hydrologic factors such as precipitation, evapotranspiration, and ground water flow. Traditional wetland mapping methods which rely on aerial photograph interpretation and simple classification techniques have several disadvantages: they are typically based on single-date imagery, are often several years old, may not be representative of the current state of the environment, and do not take into account the seasonal nature of wetland boundaries. Such traditional maps are not reliable for two particular wetland types: forested and ephemeral.

Separating forested wetlands from forested uplands with optical imagery is problematic because the imagery, even if collected during leaf-off conditions, may not reveal the underlying hydrology of a site. The collection of optical imagery can also be hindered by cloud cover (Baker, Lawrence, Montagne, & Patten, 2006; E. W. Ramsey, 1995; E. W. Ramsey et al., 1998; Töyrä, Pietroniro, Martz, & Prowse, 2002), thus potentially missing a critical period for ephemeral wetland assessment.

Radar imagery may provide a solution to traditional wetland mapping concerns. In areas of frequent cloud cover, optical imagery has an obvious disadvantage. Long wave radar signals, on the other hand, are not sensitive to the atmosphere, nor require daylight hours for acquisition, and thereby increase the possibility for frequent and quality data collection (Parmuchi, Karszenbaum, & Kandus, 2002; Townsend, 2001). A review of radar detection of wetlands by Henderson & Lewis (2008) illustrates the complexity and dependence on local environmental conditions for wetland mapping accuracy.

Wetland maps made using satellite imagery with larger spectral and spatial resolution incorporate more information about surface characteristics. Empirical models can be developed to estimate soil moisture and potential wetness, thus increasing the feasibility of differentiating between a broad range of wetland types (Arzandeh & Wang, 2002; Li & Chen, 2005; Ozesmi & Bauer, 2002; E. W. Ramsey, Nelson, & Sapkota, 1998). There are many different methods to use radar imagery to map wetlands; however, the classification technique which is the most accurate may not always be the most feasible.

Rule-based classifiers require prior knowledge about the surface properties such as: radar speckle and radar backscattering effects from changes in soil moisture and dielectric properties of vegetation and soil (Kasischke et al., 2003; Parmuchi et al., 2002). On the other hand, object-based classifiers take into account neighboring pixels to classify segments of homogeneous boundaries using measures such as texture, shape, pattern, size, as well spectral-radiometric information. This method is also called image segmentation and is computationally expensive (Grenier et al., 2007; Harken & Sugumaran, 2005; Stuckens, Coppin, & Bauer, 2000).

Evaluation is needed of multiple combinations of input datasets and classification techniques in order to strike a balance between accuracy, economic and feasibility. Using radar imagery and modern classification techniques, the accuracy of locating and differentiating between wetland types is increased and the time it would traditionally take to map difficult wetland types is significantly reduced.

#### **2.4.2 Planned Methodology**

A series of comparisons will be drawn from the results of several classification techniques with the following data inputs: different types of radar imagery, high resolution topography and potential wetness models, soil survey maps, and leaf-on and leaf-off optical imagery. Accuracy will be assessed by utilizing ground reference data from pilot sites. Evaluation of the results will ultimately be used to design a recommendation for the most effective and feasible wetland mapping statewide.

The mapping methods discussed here will utilize Radarsat-2 and PALSAR imagery (C- and L-bands, 5.66 cm and 23.5 cm wavelength, respectively). The dynamic nature of wetland areas will be explored by acquiring imagery for three dates per year (May, July, and September) in pilot study areas over a two year period. Radar backscatter directly relates to the surface properties and the spectral band utilized. Longer wavelengths are more able to penetrate through rough or densely vegetated surfaces and reach the soil surface (Campbell, J.B, 2007). The C and L wavelengths will be evaluated for accuracy in mapping forested wetlands.

The radar images will be acquired with varying signal polarizations (horizontal-horizontal, HH; vertical-vertical, VV; horizontal-vertical, HV; and vertical-horizontal, VH). Polarization signifies the orientation of the energy transmitted or received by the radar antenna, which is directly related to the physical and electrical properties of surface features (Campbell, J.B, 2007). Combinations of polarizations have been shown to detect vegetation differences and differentiate between ground cover types reasonably well (Baghdadi, Bernier, Gauthier, & Neeson, 2001; Henderson & Lewis, 2008; Slatton, Crawford, & Chang, 2008). Polarization, wavelength, and combinations thereof, will be evaluated for accuracy in differentiating various wetland types.

Provided resources for field data collection are available, relationships between measured soil moisture and backscatter or polarization effects will be developed to estimate soil moisture with remotely sensed data. Soil moisture maps are important for identifying the hydrology of an area. Using empirical models, the differentiation between a broader range of wetland types is possible (Arzandeh & Wang, 2002; Li & Chen, 2005; Ozesmi & Bauer, 2002; E. W. Ramsey, Nelson, & Sapkota, 1998). If resources are not available or feasible, other empirical models found in the literature for estimating soil moisture with radar imagery will be explored.

The reference data will be collected from randomly distributed points (the minimum number of points for statistical significance is to be determined), generated within both pilot study areas. The reference points will be revisited at least three times per season over two years of this project (during times coincident with radar image acquisition). The field procedures will involve locating and physically visiting each point with a GPS unit, identifying the dominant wetland type and taking notes on vegetation species, approximating the ground cover density, measuring the soil moisture content within a specific area surrounding the point (to be determined) using a time domain reflectometry (TDR) soil moisture probe, and taking representative photographs. This intensive field work will determine how soil moisture and other observed characteristics change seasonally, from year to year, and within different wetland types.

The classification techniques that will be explored include: a) supervised classification with combined optical and radar imagery and using ground reference data as training for the classifier algorithm; b) image segmentation using combined optical and radar imagery; and c) wetland probability maps, using decision tree classifier with combined optical and radar imagery and soil moisture measured in the field pilot study areas.

Each of the above classification techniques for wetland mapping will be compared to traditional methods and the relative feasibility of each technique will be determined. Accuracy assessment results will show which method offers both the highest accuracy for specific wetland types and the most feasible implementation for large geographical areas. The final results will be used to develop a recommendation for the most cost-effective and reliable statewide wetland mapping.

### 2.4.3 Expected Results

Results from this research will substantially improve the information available to wetland mapping personnel and those charged with identifying restorable wetlands, mapping ecosystem function, and quantifying wetland change. This additional information is expected to save time and money for mapping wetlands that are traditionally difficult to map, such as forested and ephemeral wetlands. The seasonal behavior of different wetland types will be better understood by monitoring both the effects of radar backscatter via multi-temporal imagery and actual soil moisture content measured on the ground in pilot study areas.

Empirical models of radar-derived soil moisture will be used to determine the seasonal and inter-annual surface water cycle dynamics of the study sites. Existing approaches for determining soil moisture from radar data will be evaluated (Kasischke et al., 2003; Lu et al., 2005; Zribi & Dechambre, 2003). This research will also seek to develop new techniques to decouple the soil moisture signal from vegetation in order to differentiate between more wetland types (Frappart, Seyler, Martinez, León, & Cazenave, 2005; E. Ramsey, Rangoonwala, Middleton, & Lu, 2009).

The following specific questions will be answered by this research: 1) How can radar imagery improve mapping accuracy of two important wetland types found in Minnesota: forested and ephemeral wetlands; 2) What are the data requirements for maximizing classification accuracy and which method has the most reliable results; and 3) What is the feasibility, both economic and operational, of statewide application of each classification method.

Research has shown that combining data from multiple sources and sensors can increase the overall accuracy of wetland classification results anywhere from 15-20% (Baker, Lawrence, Montagne, & Patten, 2006; E. W. Ramsey, 1995; E. W. Ramsey et al., 1998; Töyrä, Pietroniro, Martz, & Prowse, 2002). Though data acquisition for this research will be relatively expensive and the evaluation of all of the wetland mapping methods with multiple input data types will be computationally intensive, there may be a significant cost savings in the end due to the time savings compared to traditional heads-up digitizing.

Instead of starting off with a single image and manually delineating boundaries, information about surface features is gathered from multiple types of data (optical, radar, topographical, soil survey) and used in a classifying algorithm. Ground reference data in pilot study areas will aid in both in the implementation of the classification and accuracy assessment of the results. The resulting wetland map can be given to wetland mapping professionals as an aid in traditional heads-up digitizing, especially for the notoriously difficult to map wetlands.

Challenges remain in implementing the new classification techniques, particularly in terms of the underused input data such as radar imagery and high resolution topographic data. Research has been done on the observed backscatter and speckle from radar data as a function of the sub-canopy vegetation, surface dielectric properties, and surface orientation with respect to the satellite (Wdowski et al., 2008; Zribi & Dechambre, 2003). More information is needed on the effects of polarization, radar signal pulse and magnitude, and soil moisture content effects on radar backscatter.

### 2.4.4 RADAR Summary and Conclusions

Results from the classification techniques and combinations of input data explored in this research will

contribute to the field of wetland science and management significantly. By starting off broad and evaluating several different methods, the scope can be narrowed in on the most feasible and accurate technique.

In this research, surface hydrologic cycle dynamics, as measured by multi-temporal satellite-based radar image data, will be examined. This data will be used in conjunction with optical imagery and other ancillary data (e.g. soil survey data and topographical models) to develop innovative mapping methods to locate and classify difficult to map wetlands (e.g. ephemeral and forested wetlands). These methods will be tested using ground reference data and are expected to achieve mapping accuracies higher than those achieved using existing traditional methods.

Ultimately, this research will produce the following: needed testing of new radar technologies, methods for more frequent and more accurate wetland mapping for monitoring purposes, much needed data on the hydrologic cycle dynamics of wetlands, and better information about water retention in wetland landscapes.

## 2.5. Field Wetland Data Collection in Carlton County

A field data collection trip was conducted from July 12-17, 2009 in the Fond du Lac Native American reservation in Carlton County, MN. The purpose of the trip was to develop a reference data set that could be used to test the techniques developed in the wetland typing work described herein and subsequent projects. A total of 182 points (151 wetland, 31 upland) were visited. Table 8 summarizes the field sites by Cowardin Code. Figure 23 shows the site locations. Data collected included location, vegetation type(s), wetland type(s), general site description, and panoramic and canopy photos.

Table 8. Field wetland site summary by Cowardin Code

Number of Sites	Cowardin Code
5	PEM1
1	PEM2
37	PFO1
4	PFO2
42	PFO4
59	PSS1
2	PSS3

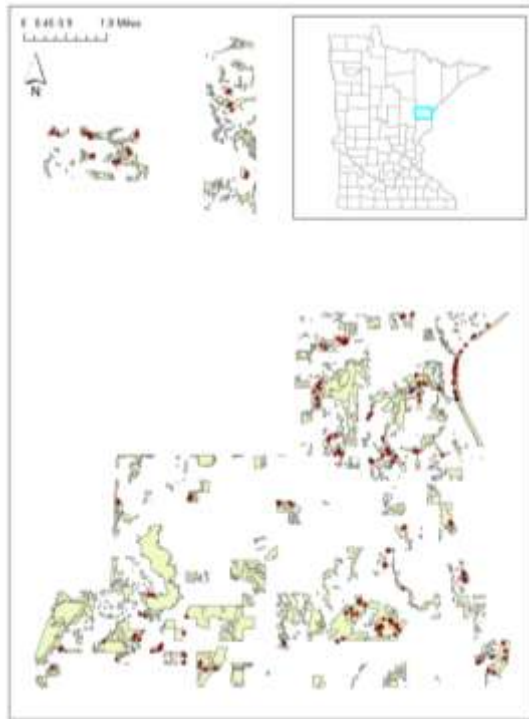


Figure 23. Left: Field sampled points (red) over wetland boundaries (tan) in Fond du Lac reservation (Carlton County, MN). Right: a wetland in the study area.

### 3. Recommendations and Protocol for Wetland Mapping in the Metro Area

#### 3.1. General Recommendations

The results presented above suggest that an ideal geospatial dataset for wetland mapping, whether for automated analysis or interpretation by analysts, would include recent high resolution color infra-red images in both leaf-on and leaf-off conditions, high resolution LIDAR data providing both a bare earth DEM and vegetation height information, RADAR image data for several dates in spring and summer, and comprehensive soil type data for the study area. The TCMA has the most geospatial data available for any location in Minnesota, but even this is not sufficient to create such an idea dataset. Thus, a wetland mapping approach for the TCMA must identify the most useful of the available data types and analysis approaches. The following are general recommendations for conducting an NWI update in the TCMA:

- *Base image data for interpretation:* 2008 NAIP 1 meter color infra-red imagery. NAIP imagery was collected in Minnesota in 2009 but it does not have a color infra-red band. An important characteristic of infra-red images is that water and saturated areas appear significantly darker than non-wet areas because of the absorption of infra-red wavelengths by water. Thus, while the 2009 NAIP images are newer and will provide a more recent wetland map, the spectral information present in the 2008 images is likely to be more advantageous in both manual interpretation and image segmentation.
- *Ancillary image data:* 2009 NAIP. The new NAIP could be viewed side-by-side with the 2009 images, providing improved spectral and temporal information.

- *Elevation data*: LIDAR DEMs where available (soon to be statewide), National Elevation Data in LIDAR coverage gaps. Elevation data are critical for identifying depressional areas that may not be readily visible on optical imagery.
- *Soils data*: NRCS SSURGO layers. The SSURGO database, while at relatively coarse spatial resolution, provides useful information about the general soil characteristics of an area. Parameters drawn from the database, such as hydric and poorly-drained designations and soil acidity data, can be used to distinguish some commonly confused wetland types – particularly in the Eggers and Reed classification system.
- *Image preprocessing*: The base image data should be segmented using an object oriented algorithm prior to interpretation. While very time consuming initially, creating image segments will substantially reduce manual interpretation time and subjectivity in drawing wetland polygon boundaries.
- *Classification system*: The Cowardin classification system should be the main wetland typing method used; however, the Eggers and Reed type for each wetland should be identified during the interpretation process. Increasing nationwide adoption of the Eggers and Reed indicates that failing to collect such data would be a substantial oversight – particularly given the difficulty of developing a robust crosswalk between Cowardin and Eggers and Reed.

## 3.2. Mapping Protocol

The following is a set of detailed guidelines and protocol steps for mapping wetlands in the TCMA. The project steps are presented in order: data acquisition, pre-interpretation data processing, data display and interpretation, post processing, delivery, and quality control.

### 3.2.1 Data Types and Software

The following data types should be acquired for use in this project:

- 2008 National Agriculture Imaging Program (NAIP) images for the study area
- 2009 National Agriculture Imaging Program (NAIP) images for the study area
- Spring leaf-off imagery
- USDA NRCS Soil Survey Geographic (SSURGO) soils data
- High resolution LiDAR DEMs where available
- National Elevation Data at 10 meter spatial resolution
- Metro counties contour maps
- MN DNR hydrology dataset (rivers, lakes, etc.)
- Optical images from other years as desired (e.g. 2005 Mark Hurd)
- USGS quarter quadrangle tile index from MN DNR
- Minnesota ecoregions layer from MN DNR

Software:

- ESRI ArcGIS
- Definiens Server 7 (or later)
- Python GDAL library
- TauDEM hydrology extension for ArcGIS

### 3.2.2 Preprocessing

- If necessary, prepare the summer aerial imagery and any available spring leaf-off imagery (all four bands) for image segmentation by splitting them into quarter quadrangle tiles using the tile index. This can be automated using Python and the GDAL library.
- Use the batch feature in Definiens to automate segmentation of the NAIP tiles using the following parameters:
  - Color/shape: 0.5 each
  - Scale 50-70 (lower for smaller wetlands)
- Generalize segment boundaries by a reasonable amount to reduce the number of vertices. This will make subsequent editing of segment boundaries much easier and will not significantly affect the segments shapes.
- Export segments from Definiens as ArcGIS Shapefiles. Ensure they are exported with projection/coordinate information.
- Create a Normalized Difference Vegetation Index layer from the NAIP infra-red and red bands
- Threshold the NDVI layer to include only pixels with values greater than 0.2
- Use the LiDAR or NED elevation layers to create a Compound Topographic Index layer using the d-infinity water flow algorithm in TauDEM
- Compute a rudimentary wetland likelihood map by using a Boolean “AND” operator with the CTI, SSURGO, and NDVI as input, where a pixel is identified as a wetland only if the CTI is above an appropriate threshold (we suggest ~11), the NDVI is above 0.2, and the soil type is either Hydric or Poorly Drained. This likelihood map is intended to assist the interpreter in identifying areas that may be wetlands, not to replace the interpreter.

### 3.2.3 Data display and Interpretation

- We recommend against viewing the old NWI polygons at any point in this procedure so as not to bias the results. The old NWI could perhaps be used after the initial interpretation as a comparison.
- A dual monitor setup is recommended if possible.
- Display in ArcGIS or other appropriate software the NAIP tile of interest, the wetland likelihood map, a topography layer (LiDAR, NED), and the image segments.
- Display NAIP images and segments for each adjacent NAIP tile so that local context can be used to inform the interpretation process at the edges of the tile of interest.
- For each segment:
  - Determine whether it is wetland or upland using the interpreter’s best professional judgment.
  - If the segment is wetland, record the Cowardin and Eggers & Reed (E&R) types in the ArcGIS table associated with the segment layer. We recommend this be done using a constrained attribute domain to minimize data entry errors.
  - Edit the boundaries of the segment using the ArcGIS feature editing tools so that the boundaries correspond to the natural wetland edges.

### 3.2.4 Data Post-processing and Delivery

- Dissolve (merge) adjacent segments that have the same wetland type. This operation should not be done if the E&R types are different.
- Delete upland segments from the segment layer.
- Deliver final segment layer as NWI wetland map. The map should be delivered at a scale desired by MN DNR, either at the quarter quad, full quad, or county, and in a GIS format such as a geodatabase.

- The product should be fully compliant with all USFWS requirements so that it is ready for upload to the main NWI.

### **3.2.5 Quality Assurance / Quality Control**

- The mapping contractor should perform comprehensive in-house validation of the data products both during and subsequent to interpretation work. These should include positional and thematic accuracy assessments.
- If a free text data entry approach is used (e.g. the interpreters type in rather than select Cowardin codes for wetland segments), attribute validity checks should be used to ensure consistency.

## **4. Conclusions**

The research presented in this document is an in-depth analysis of selected wetland mapping techniques for the TCMA. While some work remains to be completed, such as the wetland typing using decision trees approach, the results are sufficient to draw conclusions and to make recommendations for the optimal approach to accomplishing the objectives of the Minnesota NWI update. The protocol provided above is expected to be suitable for meeting or exceeding the FGDC wetland mapping standard and thus allowing for the inclusion of Minnesota's updated wetland maps in the USFWS National Wetland Inventory.

## 5. References

- Arzandeh, S., & Wang, J. (2003). Monitoring the change of *phragmites* distribution using satellite data. *Canadian Journal of Remote Sensing*, 29(1), 24-35.
- Baghdadi, N., Bernier, M., Gauthier, R., & Neeson, I. (2001). Evaluation of C-band SAR data for wetlands mapping. *International Journal of Remote Sensing*, 22(1), 71-88.
- Baker, C., Lawrence, R., Montagne, C., & Patten, D. (2006). Mapping wetlands and riparian areas using Landsat ITM+ imagery and decision-tree-based models. *Wetlands*, 26(2), 465-474.
- Becker, B. L., Lusch, D. P., & Qi, J. (2005). Identifying optimal spectral bands from in situ measurements of great lakes coastal wetlands using second-derivative analysis. *Remote Sensing of Environment*, 97(2), 238-248.
- Becker, B. L., Lusch, D. P., & Qi, J. (2007). A classification-based assessment of the optimal spectral and spatial resolutions for great lakes coastal wetland imagery. *Remote Sensing of Environment*, 108(1), 111-120.
- Blyth E. M., Finch J., Robinson M., Rosier P.: Can soil moisture be mapped onto the terrain? *Hydrology and Earth System Sciences* 8 (2004) 923-93
- Bolstad, P. V., & Lillesand, T. M. (1992). Improved classification of forest vegetation in northern Wisconsin through a rule-based combination of soils, terrain, and Landsat Thematic Mapper data. *Forest Science*, 38(1), 5-20.
- Bolstad, Paul (2006); "GIS Fundamentals", second edition, [www.paulbolstad.net/gisbook.html](http://www.paulbolstad.net/gisbook.html)
- Bourgeau-Chavez, L. L., Kasischke, E. S., Brunzell, S. M., Mudd, J. P., Smith, K. B., & Frick, A. L. (2001). Analysis of space-borne SAR data for wetland mapping in Virginia riparian ecosystems. *International Journal of Remote Sensing*, 22(18), 3665.
- Bruzzone, L. and Carlin, L. 2006. A multilevel context-based system for classification of very high spatial resolution images. *IEEE Transactions on Geoscience and Remote Sensing*, 44(9): 2587-2600.
- Campbell, J.B. 2007. *Introduction to Remote Sensing*. 4th edition. The Guilford Press: New York, NY
- Costa, M. P. F., & Telmer, K. H. (2006). Utilizing SAR imagery and aquatic vegetation to map fresh and brackish lakes in the Brazilian pantanal wetland. *Remote Sensing of Environment*, 105(3), 204-213.
- Costa-Cabral, M. and Burges, S. J. (1994). Digital Elevation Model Networks (DEMON): A Model of Flow Over Hillslopes for Computation of Contributing and Dispersal Areas. *Water Resources Research*, 30(6): 1681-1692
- Cowardin, L. M., & Myers, V. I. (1974). Remote sensing for identification and classification of wetland vegetation. *The Journal of Wildlife Management*, 38(2), 308-314.

Cowardin, L. M., Carter, V., Golet, F. C., & LaRoe, E. T. (1974). Classification of wetlands and deepwater habitats of the United States.

Craig Dobson, M., Ulaby, F. T., & Pierce, L. E. (1995). Land-cover classification and estimation of terrain attributes using synthetic aperture radar. *Remote Sensing of Environment*, 51(1), 199-214.

Creed, I. F., Sanford, S. E., Beall, F. D., Molot, L. A., & Dillon, P. J. (2003). Cryptic wetlands: Integrating hidden wetlands in regression models of the export of dissolved organic carbon from forested landscapes. *Hydrological Processes*, 17(18), 3629-3648.

Dahl, T. E. (1990). *Wetlands losses in the united states 1780's to 1980's*. Washington, D.C.: U.S. Department of the Interior, Fish and Wildlife Service.

Dahl, T. E., & Johnson, C. E. (1991). *Status and trends of wetlands in the conterminous United States, mid-1970's to mid-1980's*. Washington, D.C.: U.S. Department of the Interior, Fish and Wildlife Service.

Definiens AG. 2006. Definiens Professional 5 Reference Book. Trappentreustr, 1D-80339 München, Germany.

Douglas, D. H. 1986. Experiments to locate ridges and channels to create a new type of digital elevation model. *Cartographic* 23: 29-61

Eggers, S.D., Reed, D.M., 1997. Wetland plants and communities of Minnesota and Wisconsin. U.S. Army Corps of Engineers, St. Paul District, 263pp.

U.S. Army Corps of Engineers. (1987). *Corps of engineers wetlands delineation manual* No. Technical Report Y-87-1). Vicksburg, Miss.: U.S. Army Engineer Waterways Experiment Station.

ERDAS IMAGINE Expert Classifier, 2005. Leica Geosystems GIS and Mapping, LLC, <http://gis.leica-geosystems.com>.

Federal Geodetic Data Committee (FGDC) Wetlands Subcommittee. 2008. FGDC draft wetlands mapping standard. Environmental Protection Agency, Office of Water.

Federal Register. (1980). 40 CFR part 230: Section 404(b)(1) guidelines for specification of disposal sites for dredged or fill material.45(249), 85352-85353.

Federal Register. (1982). Title 33: Navigation and navigable waters; chapter II, regulatory programs of the corps of engineers. 47(138), 31810.

Fournier, Grenier, Lavoie, & Helie, 2007. Towards a strategy to implement the Canadian Wetland Inventory using satellite remote sensing.

Frappart, F., Seyler, F., Martinez, J., León, J. G., & Cazenave, A. (2005). Floodplain water storage in the negro river basin estimated from microwave remote sensing of inundation area and water levels. *Remote Sensing of Environment*, 99(4), 387-399. doi:DOI: 10.1016/j.rse.2005.08.016

Grenier, M., Demers, A. M., Labrecque, S., Benoit, M., Fournier, R. A., & Drolet, B. (2007). An object-based method to map wetland using RADARSAT-1 and Landsat ETM images: Test case on two sites in Quebec, Canada. *Canadian Journal of Remote Sensing*, 33(Suppl. 1), S28-S45.

Grenier, M., Demers, A., Labrecque, S., Benoit, M., Fournier, R.A., and Drolet, B. 2007. An object-based method to map wetland using Radarsat-1 and Landsat ETM imagers: test case on two sites in Quebec, Canada. *Canadian Journal of Remote Sensing*. 33 (Suppl. 1), S28-S45.

Guntner A., Seibert J., Uhlenbrook S.: Modeling spatial patterns of saturated areas: An evaluation of different terrain indices. *Water Resources Research* 40 (2004) W05114

Harken, J., & Sugumaran, R. (2005). Classification of iowa wetlands using an airborne hyperspectral image: A comparison of the spectral angle mapper classifier and an object-oriented approach. *Canadian Journal of Remote Sensing*, 31(2), 167-174.

Harvey, K. R., & Hill, G. J. E. (2001). Vegetation mapping of a tropical freshwater swamp in the Northern Territory, Australia: A comparison of aerial photography, landsat TM and SPOT satellite imagery. *International Journal of Remote Sensing*, 22(15), 2911.

Healy, T. (2005). *Muddy coasts*

Henderson, F. M., & Lewis, A. J. (2008). Radar detection of wetland ecosystems: A review. *Int.J.Remote Sens.*, 29(20), 5809-5835.

Hess, L. L., Melack, J. M., & Simonett, D. S. (1990). Radar detection of flooding beneath the forest canopy: A review. *International Journal of Remote Sensing*, 11(7), 1313.

Hess, L. L., Melack, J. M., Filoso, S., & Yong Wang. (1995). Delineation of inundated area and vegetation along the Amazon floodplain with the SIR-C synthetic aperture radar. *Geoscience and Remote Sensing, IEEE Transactions on*, 33(4), 896-904.

Hess, L. L., Melack, J. M., Novo, E. M. L. M., Barbosa, C. C. F., & Gastil, M. (2003). Dual-season mapping of wetland inundation and vegetation for the central amazon basin. *Remote Sensing of Environment*, 87(4), 404-428.

Hirano, A., Madden, M., & Welch, R. (2003). Hyperspectral image data for mapping wetland vegetation. *Wetlands*, 23(2), 436-448.

Hodgson, M. E., Jensen, J. R., Mackey, H. E., & Coulter, M. C. (1987). Remote sensing of wetland habitat: A wood stork example. *Photogrammetric Engineering and Remote Sensing*, 53, 1075-1080.

Huan, Y. and Zhang, S. 2008. Application of high resolution satellite imagery for wetlands cover classification using object-oriented method. *The International Archives of the Photogrammetry, Remote Sensing and Spatial Information Sciences*. 37(B7): 521-526.

Hunt, R., Hamilton, R., and Everitt, J. 2007. Mapping weed infestations using remote sensing, in *A Weed Manager's Guide to Remote Sensing and GIS – Mapping and Monitoring*, USDA Forest Service.

Islam, Md.A., Thenkabail, P.S., Kulawardhana, R.W., Alankara, R., Gunasinghe, S., Edussriya, C., et al. (2008). Semi-automated methods for mapping wetlands using Landsat ETM+ and SRTM data. *Int. J. Remote Sens.*, 29(24), 7077-7106.

Jensen, John R., 2005, *Introductory Digital Image Processing*, 3rd Ed., Upper Saddle River, NJ: Prentice Hall, 526 pages.

Johnston, C. A. (1989). *Human impacts to Minnesota wetlands* No. PB-91-183160/XAB; EPA--600/J-89/519). Duluth, Minnesota: U.S. Environmental Protection Agency.

Kasischke, E. S., Melack, J. M., & Craig Dobson, M. (1997). The use of imaging radars for ecological applications - a review. *Remote Sensing of Environment*, 59(2), 141-156.

Kasischke, E. S., Smith, K. B., Bourgeau-Chavez, L. L., Romanowicz, E. A., Brunzell, S., & Richardson, C. J. (2003). Effects of seasonal hydrologic patterns in south Florida wetlands on radar backscatter measured from ERS-2 SAR imagery. *Remote Sensing of Environment*, 88(4), 423-441. doi:DOI: 10.1016/j.rse.2003.08.016

Kloiber, S. Personal communication, 1/4/2010.

Lang, M.W. and G.W. McCarty, 2009. Lidar intensity for improved detection of inundation below the forested canopy. *Wetlands* 29(4).

Li, J., & Chen, W. (2005). A rulebased method for mapping canada's wetlands using optical, radar and DEM data. *International Journal of Remote Sensing*, 26, 5051-5069(19).

Li, J., & Chen, W. (2005). A rule-based method for mapping Canada's wetlands using optical, radar and DEM data. *International Journal of Remote Sensing*, 26(22), 5051-5069.

Lozano-Garcia, D. F., & Hoffer, R. M. (1993). Synergistic effects of combined Landsat-TM and SIR-B data for forest resources assessment. *International Journal of Remote Sensing*, 14(14), 2677.

Lu, Z., Crane, M., Kwoun, O., Wells, C., Swarzenski, C., & Rykhus, R. (2005). C-band radar observes water level change in swamp forests. EOS, TRANSACTIONS AMERICAN GEOPHYSICAL UNION, 86(14)

Meinel, G. and M. Neubert. 2004. A comparison of segmentation programs for high resolution remote sensing data. *International Archives of Photogrammetry and Remote Sensing*, XXXV(Part B): 1097-1105.

Moore, I. D., O'Loughlin, E. M., & Burch, G. J. (1988). A contour-based topographic model for hydrological and ecological applications. *Earth Surface Processes and Landforms*, 13(4), 305-320.

Moore, I. D., R. B. Grayson, and A. R. Ladson. 1991. Digital terrain modeling: a review of hydrological, geomorphological, and biological applications. *Hydrological Processes* 5:3-30

Murphy, P. N. C., Ogilvie, J., Connor, K., & Arp, P. A. (2007). Mapping wetlands: a comparison of two different approaches for New Brunswick, Canada. *Wetlands*, 27(4), 846-854.

- Neuenschwander, A. L., Crawford, M. M., & Provanca, M. J. (1998). *Mapping of coastal wetlands via hyperspectral AVIRIS data*
- Ozesmi, S. L., & Bauer, M. E. (2002). Satellite remote sensing of wetlands. *Wetlands Ecology and Management*, 10(5), 381-402.
- Parmuchi, M. G., Karszenbaum, H., & Kandus, P. (2002). Mapping wetlands using multi-temporal RADARSAT-1 data and a decision-based classifier. *Canadian Journal of Remote Sensing*, 28(2), 175-186.
- Ramsey III, E. W. (1998). Radar remote sensing of wetlands. In R. Lunetta, & C. Elvidge (Eds.), *Remote sensing change detection: Environmental monitoring methods and applications* (pp. 211-243). Ann Arbor, MI: Ann Arbor Press Inc.
- Ramsey, E. W. (1995). Monitoring flooding in coastal wetlands by using radar imagery and ground-based measurements. *International Journal of Remote Sensing*, 16(13), 2495.
- Ramsey, E. W., Nelson, G. A., & Sapkota, S. K. (1998). Classifying coastal resources by integrating optical and radar imagery and color infrared photography. *Mangroves and Salt Marshes*, 2(2), 109-119. Retrieved from <http://dx.doi.org.floyd.lib.umn.edu/10.1023/A:1009911224982>
- Ramsey, E., Ragoonwala, A., Middleton, B., & Lu, Z. (2009). Satellite optical and radar data used to track wetland forest impact and short-term recovery from Hurricane Katrina. *Wetlands*, 29(1), 66-79. doi:10.1672/08-103.1
- Repaka, S.R., Truax, D. D., Kolstad, E., and O'Hara, C. G. 2004. Comparing spectral and object based approaches for classification and transportation feature extraction from high resolution multispectral imagery, in *Proceedings form ASPRS Annual Conference*.
- Rosenqvist, A., Shimada, M., Chapman, B., McDonald, K., De Grandi, G., Jonsson, H., et al. (2004). *An overview of the JERS-1 SAR global boreal forest mapping (GBFM) project*
- Sader, S. A., Ahl, D., & Liou, W. (1995). Accuracy of Landsat-TM and GIS rule-based methods for forest wetland classification in Maine. *Remote Sensing of Environment*, 53(3), 133-144.
- Shaw, Samuel P. and C. Gordon Fredine 1956. *Wetlands of the United States - their extent and their value to waterfowl and other wildlife*. U.S. Department of the Interior, Washington, D.C. Circular 39. 67pp.
- Shuman, C. S., & Ambrose, R. F. (2003). A comparison of remote sensing and ground-based methods for monitoring wetland restoration success. *Restoration Ecology*, 11(3), 325-333.
- Slatton, K. C., Crawford, M. M., & Chang, L. D. (2008). Modeling temporal variations in multipolarized radar scattering from intertidal coastal wetlands. *ISPRS Journal of Photogrammetry and Remote Sensing*, 63(5), 559-577. doi:DOI: 10.1016/j.isprsjprs.2008.07.003
- Stuckens, J., Coppin, P. R., & Bauer, M. E. (2000). Integrating contextual information with per-pixel classification for improved land cover classification. 71(6), 282-296.

Tarboton, D. G. 1997. A new method for the determination of flow directions and upslope areas in grid digital elevation models. *Water Resources Research* 33: 309-319

Thompson, J. A., Bell, J. C., & Butler, C. A. (2001). Digital elevation model resolution: Effects on terrain attribute calculation and quantitative soil-landscape modeling. *Geoderma*, 100(1-2), 67-89.

Tiner Jr., R. W. (1990). Use of high-altitude aerial photography for inventorying forested wetlands in the United States. *Forest Ecology and Management*, 33-34, 593-604.

Townsend, P. A. (2001). Mapping seasonal flooding in forested wetlands using multi-temporal radarsat SAR. *Photogrammetric Engineering & Remote Sensing*, 67(7), 857-864.

Townsend, P., & Walsh, S. (2001). Remote sensing of forested wetlands: Application of multitemporal and multispectral satellite imagery to determine plant community composition and structure in southeastern USA. *Plant Ecology*, 157(2), 129-149.

Töyrä, J., Pietroniro, A., Martz, L. W., & Prowse, T. D. (2002). A multi-sensor approach to wetland flood monitoring. *Hydrological Processes*, 16(8), 1569-1581.

Wang, J., Shang, J., Brisco, B., & Brown, R. J. (1998). Evaluation Of multi-date ERS-1 and multispectral Landsat imagery for wetland detection in southern Ontario. *Canadian Journal of Remote Sensing*, 24(1), 60-68.

Wang, J., Zheng, L., & Tong, Q. (1998). Derivative spectra matching for wetland vegetation identification and classification by hyperspectral image. 3502(1) 280-288.

Wang, Y., Hess, L. L., Filoso, S., & Melack, J. M. (1995). Understanding the radar backscattering from flooded and non-flooded Amazonian forests: Results from canopy backscatter modeling. *Remote Sensing of Environment*, 54(3), 324-332.

Wdowinski, S., Kim, S., Amelung, F., Dixon, T. H., Miralles-Wilhelm, F., & Sonenshein, R. (2008). Space-based detection of wetlands' surface water level changes from L-band SAR interferometry. *Remote Sensing of Environment*, 112(3), 681-696.

Whitcomb, J., Moghaddam, M., McDonald, K., Podest, E., & Kelldorfer, J. (2007). *Wetlands map of alaska using L-band radar satellite imagery*

Wright, C., & Gallant, A. (2007). Improved wetland remote sensing in Yellowstone National Park using classification trees to combine TM imagery and ancillary environmental data. *Remote Sensing of Environment*, 107(4), 582-605.

Zribi, M., & Dechambre, M. (2003). A new empirical model to retrieve soil moisture and roughness from C-band radar data. *Remote Sensing of Environment*, 84(1), 42-52. doi:DOI: 10.1016/S0034-4257(02)00069-X